H2Bub1 Regulates *RbohD*-Dependent Hydrogen Peroxide Signal Pathway in the Defense Responses to *Verticillium dahliae* Toxins[1]

Jun Zhao,[2] Qiuhong Chen,[2] Sa Zhou,[3] Yuhui Sun, Xinyue Li, and Yingzhang Li[4,5]

State Key Laboratory of Plant Physiology and Biochemistry, College of Biological Sciences, China Agricultural University, Beijing 100193, China

ORCID ID: 0000-0002-4795-4851 (Y.L.).

Histone H2B monoubiquitination (H2Bub1) plays critical roles in regulating growth and development as well as stress responses in Arabidopsis (*Arabidopsis thaliana*). In this study, we used wild-type and HUB1 and HUB2 loss-of-function Arabidopsis plants to elucidate the mechanisms involved in the regulation of the plant's defense responses to *Verticillium dahliae* toxins (Vd-toxins). We demonstrated that HUB-mediated H2Bub1 regulates the expression of the NADPH oxidase *RbohD* by enhancing the enrichment of histone H3 trimethylated on Lys-4 in response to Vd-toxins. *RbohD*-dependent hydrogen peroxide (H_2O_2) signaling is a critical modulator in the defense response against Vd-toxins. Moreover, H2Bub1 also affects posttranscriptional mitogen-activated protein kinase (or MPK) signaling. H2Bub1 was required for the activation of MPK3 and MPK6. MPK3 and MPK6 are involved in regulating *RbohD*-mediated H_2O_2 production. MPK3 and MPK6 are associated with protein tyrosine phosphatases (PTPs), such as Tyr-specific phosphatase1 and mitogen-activated protein kinases phosphatase1, which negatively regulated H_2O_2 production. In addition, H2Bub1 is involved in regulating the expression of *WRKY33*. WRKY33 directly binds to *RbohD* promoter and functions as a transcription factor to regulate the expression of *RbohD*. Collectively, our results indicate that H2Bub1 regulates the NADPH oxidase *RbohD*-dependent H_2O_2 production and that the PTP-MPK3/6-WRKY pathway plays an important role in the regulation of *RbohD*-dependent H_2O_2 signaling in defense responses to Vd-toxins in Arabidopsis.

Post-translational modifications of histones play key roles in regulating chromatin dynamics, gene transcription, and DNA repair. Histone H2B monoubiquitination (H2Bub1) is a key modification that has significant effects, mainly associated with transcriptional activation and elongation, on genes (Pavri et al., 2006; Weake and Workman, 2008). H2Bub1 regulates multiple developmental processes in plants, including seed dormancy, leaf and root growth (Fleury et al., 2007; Liu et al., 2007), control of flowering time, plant development (Cao et al., 2008, 2015; Gu et al., 2009; Schmitz et al., 2009; Xu et al., 2009), photomorphogenesis, and circadian rhythms (Bourbousse et al., 2012; Himanen et al., 2012). The roles of H2Bub1in flowering time and circadian rhythm regulation are associated with histone H3 trimethylated on Lys-4 (H3K4me3) and/or with H3K36me3 (Cao et al., 2008; Himanen et al., 2012; Malapeira et al., 2012; Feng and Shen, 2014; Zhao et al., 2019). Moreover, H2Bub1 is involved in the regulation of defense responses and cuticle composition, which is a defensive barrier that protects plants against biotic stresses (Dhawan et al., 2009; Ménard et al., 2014; Zou et al., 2014). However, the mechanisms of H2Bub1 in plant defense responses are not fully understood.

Verticillium dahliae is a soil-borne pathogen that causes *Verticillium* wilt in a range of important plant species worldwide (Bhat and Subbarao, 1999). Although the physiology of plant defenses against *Verticillium* infection is well established (Fradin and Thomma, 2006; Shaban et al., 2018), the molecular mechanisms and regulatory pathways involved in the defense response to *Verticillium* remain largely unknown. Hydrogen peroxide (H_2O_2) may act as an upstream signal to modulate the expression of defense genes against *V. dahliae* toxins (Vd-toxins) in Arabidopsis (*Arabidopsis thaliana*; Yao et al., 2011). H2Bub1 plays an important role in the defense response to Vd-toxins, and HUB1 and HUB2 loss-of-function plants have reduced levels of Vd-toxins-induced H_2O_2 production (Hu et al., 2014).

[1]This work was supported by the National Natural Science Foundation of China (grant nos. 31370292 and 31670252) and the National Transgenic Research Project (grant no. 2015ZX08005-002) to Y.L.

[2]These authors contributed equally to the article.

[3]Present address: Key Laboratory of Industrial Fermentation Microbiology, Ministry of Education, College of Biotechnology, Tianjin University of Science and Technology, Tianjin 300457, China.

[4]Author for contact: liyingzhang@cau.edu.cn.

[5]Senior author.

The author responsible for distribution of materials integral to the findings presented in this article in accordance with the policy described in the Instructions for Authors (www.plantphysiol.org) is: Yingzhang Li (liyingzhang@cau.edu.cn).

J.Z., Q.C., and Y.L. designed the research and wrote the article; J.Z., Q.C., S.Z., Y.S., and X.L. performed specific experiments and analyzed the data; Y.L. revised and edited the article.

www.plantphysiol.org/cgi/doi/10.1104/pp.19.00913

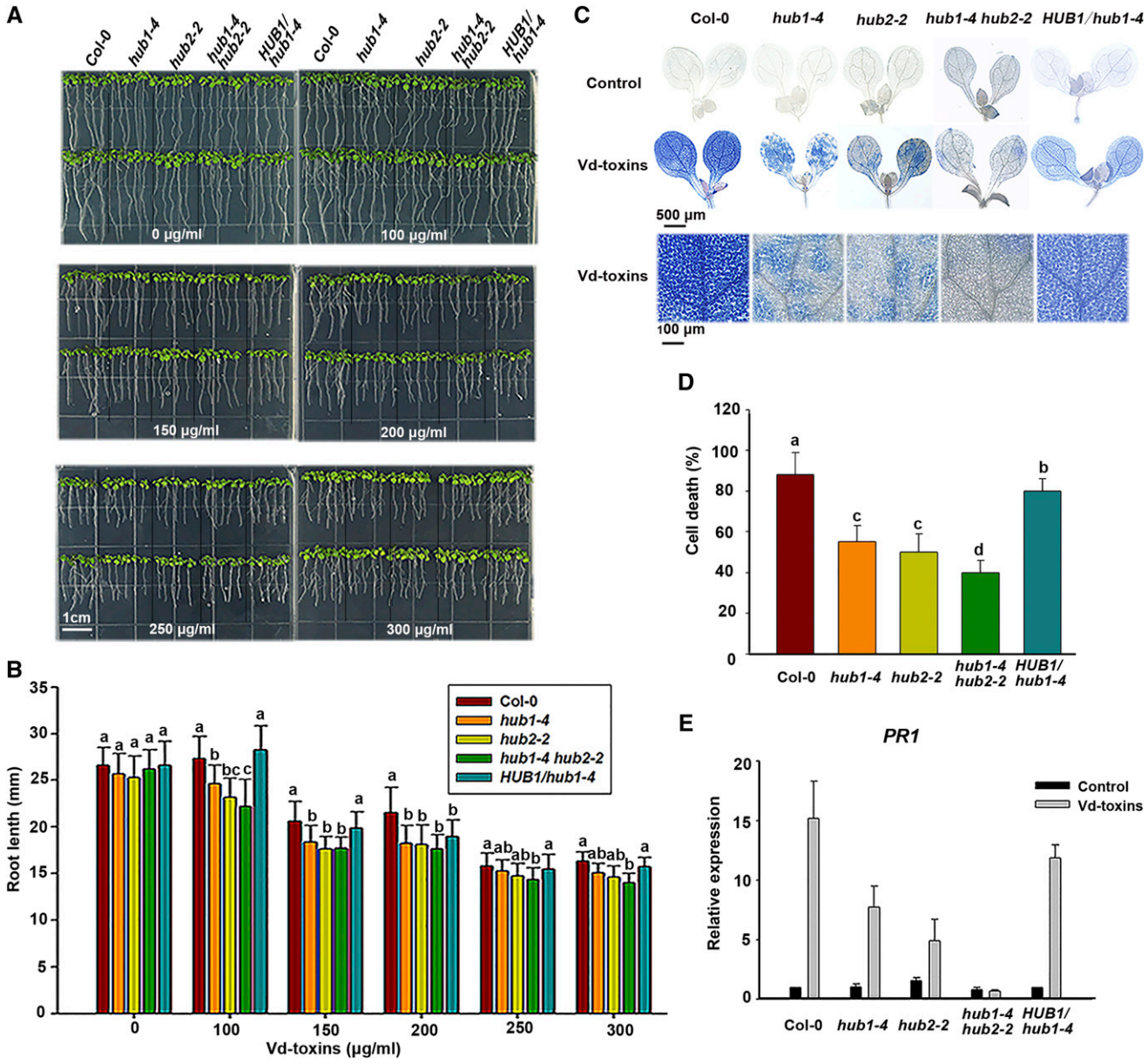

Figure 1. HUB1 and HUB2 are involved in regulating defense responses to Vd-toxins in Arabidopsis. A, Root growth of wild-type Columbia-0 (Col-0), *hub1-4*, *hub2-2*, and *hub1-4 hub2-2* mutants, and *HUB1/hub1-4* complementation line seedlings treated with Vd-toxins. Seedlings (4 d old) of the wild type and mutants were transferred from one-half-strength Murashige and Skoog (MS) medium to one-half-strength MS medium without or with Vd-toxins (100–300 μg mL^{-1}). Photographs were taken 4 d after transfer. B, Quantification of root lengths in A. Error bars indicate SD; $n = 30$. C, Vd-toxins-induced cell death in cotyledons of the Arabidopsis wild type, the *hub1-4*, *hub2-2*, and *hub1-4 hub2-2* mutants, and the *HUB1/hub1-4* complementation line. Cotyledons of 7-d-old plants were treated with 150 μg mL^{-1} Vd-toxins and stained with Trypan Blue. Leaves treated with double distilled water were used as controls. D, Quantification of the cell death rates induced by Vd-toxins in C using ImageJ software. Error bars indicate SD; $n = 8$. E, Relative expression levels of the defense gene *PR1* in the wild type, the *hub1-4*, *hub2-2*, and *hub1-4 hub2-2* mutants, and the *HUB1/hub1-4* complementation line were determined after treatment with 150 μg mL^{-1} Vd-toxins. Seedlings treated with double distilled water were used as controls. Total RNA was extracted 24 h after the Vd-toxins treatment for RT-qPCR analysis. Error bars indicate SD; $n = 15$. Different letters represent significant differences at $P < 0.05$ by one-way ANOVA with Tukey's honestly significant difference posthoc tests. All experiments were repeated at least three times.

However, the molecular mechanisms of H2Bub1 in the regulation of the defense response to Vd-toxins in plants remain unknown.

The recognition of pathogens by plants triggers several early defense responses, including the production of reactive oxygen species (ROS) and the activation of

mitogen-activated protein kinases (MAPKs; Lamb and Dixon, 1997; Torres et al., 2005; Boller and Felix, 2009). Plant NADPH oxidases, also known as respiratory burst oxidase homologs (RBOHs), are major sources of ROS during plant-pathogen interactions. *RbohD* and *RbohF* mediate diverse physiological processes, including responses to pathogens, in Arabidopsis. Both *AtRbohD* and *AtRbohF* were initially described as key components of plant defense (Torres et al., 2002; Torres and Dangl, 2005). However, they have contrasting functions in the regulation of cell death in response to pathogen attack (Torres and Dangl, 2005). *RbohD* is responsible for the generation of ROS in the response of Arabidopsis to all pathogens tested (Miller et al., 2009; Suzuki et al., 2011; Marino et al., 2012), while *AtRbohF* is a crucial modulator in the regulation of metabolic responses and resistance in Arabidopsis (Chaouch et al., 2012).

MAPK cascades play pivotal roles in defense-related signaling pathways of plants (Pedley and Martin, 2005). In Arabidopsis, three MAPKs (MPK3, MPK4, and MPK6) have been implicated in the defense against pathogens (Asai et al., 2002; Ichimura et al., 2002). MPK3 and MPK6 play positive roles in the activation of defense responses in Arabidopsis (Beckers et al., 2009; Rodriguez et al., 2010). However, the literature on the connection between MAPK activation and ROS production is contradictory. Some reports indicate that the MAPKs function downstream of the ROS burst during the triggering of plant immunity (Apel and Hirt, 2004; Pitzschke and Hirt, 2009). In contrast, other studies suggest that MAPKs act upstream of ROS production in the plant immunity-related signaling pathway (Zhang et al., 2007; Asai et al., 2008). Recently, studies have indicated that MAPK activation and the ROS burst are two independent early-signaling events in plant immunity (Segonzac et al., 2011; Xu et al., 2014).

MAPKs can be inactivated fully by MAPK phosphatases that dephosphorylate both Ser/Thr and Tyr residues (Chen et al., 2001). Tyr phosphatases play important roles in the regulation of MAPK cascades (Ichimura et al., 2002). Tyr phosphorylation plays a key role in regulating defense signaling in plants (Lin et al., 2014; Macho et al., 2014). Furthermore, protein Tyrosine Phosphatase1 (PTP1) and MAPK Phosphatase1 (MKP1), two main Tyr phosphatases, act as repressors of MPK3/MPK6-dependent stress-related signaling (Bartels et al., 2009). MKP1-mediated deactivation of

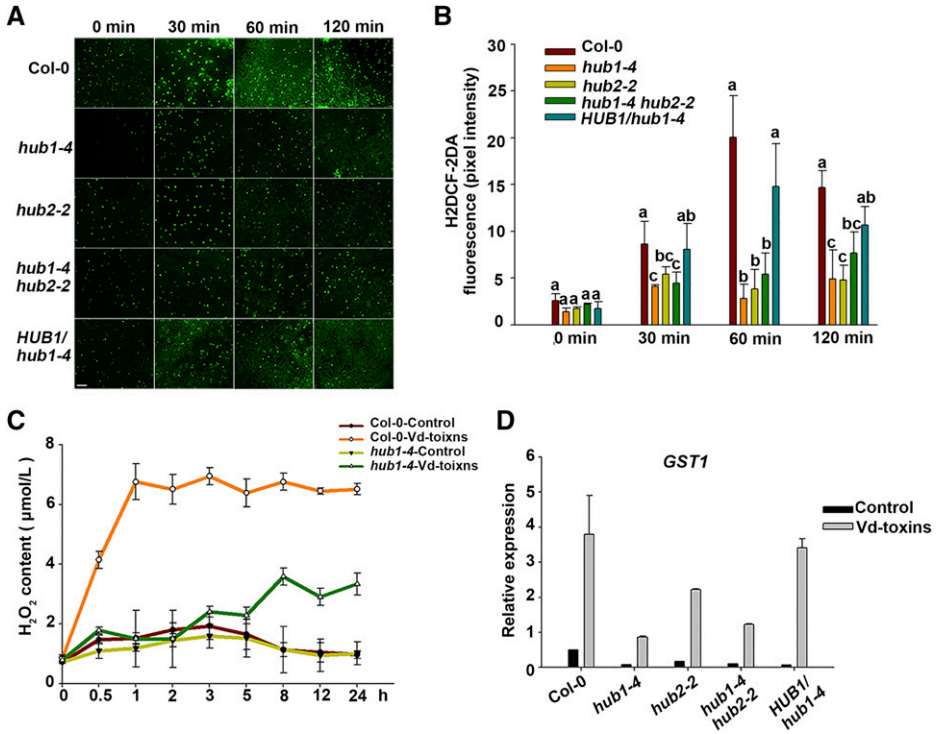

Figure 2. H_2O_2 production induced by Vd-toxins in the leaves of wild-type Arabidopsis Columbia-0 (Col-0) and mutants. A, H_2O_2 was detected by fluorescence resulting from H_2DCF-DA, as described in "Materials and Methods." Bar = 100 μm. B, Quantification of the H_2DCF-DA fluorescence intensities in A. Error bars indicate SD; $n = 8$. Different letters represent significant differences at $P < 0.05$ by one-way ANOVA with Tukey's honestly significant difference posthoc tests. C, Quantitative measurements of H_2O_2 concentrations in the leaves using the chromogenic peroxidase-coupled assay. Error bars indicate SD; $n = 3$. D, Relative expression levels of *GST1* after treatment with 150 μg mL^{-1} Vd-toxins in the wild type, the *hub1-4*, *hub2-2*, and *hub1-4 hub2-2* mutants, and the *HUB1/hub1-4* complementation line. Seedlings treated with double distilled water were used as controls. Total RNA was extracted 24 h after the Vd-toxins treatment for RT-qPCR analysis. Error bars indicate SD; $n = 3$. All experiments were repeated at least three times.

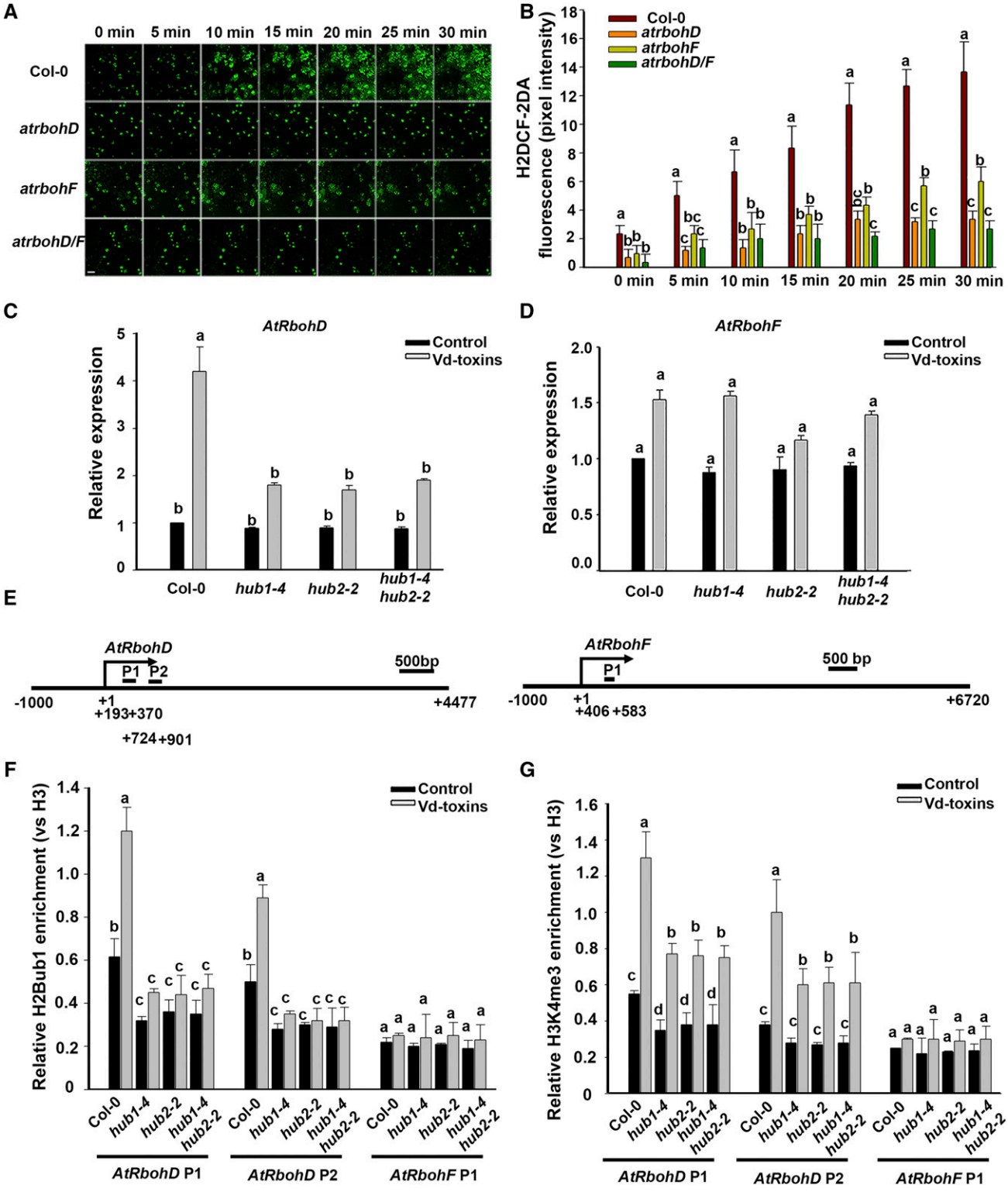

Figure 3. *AtRbohD* and *AtRbohF* expression affect H_2O_2 production and the HUB1/HUB2-regulated *AtRbohD* expression level in response to the Vd-toxins treatment in Arabidopsis. A, H_2O_2 was detected in the leaves of wild-type Columbia-0 (Col-0) and the *atrbohD*, *atrbohF*, and *atrbohD/F* mutants by assessing the fluorescence resulting from H_2DCF-DA, as described in "Materials and Methods." Bar = 20 μm. B, Quantification of the H_2DCF-DA fluorescence intensities in A. Error bars indicate SD; $n = 8$. C and D, Relative expression levels of *AtRbohD* and *AtRbohF* after treatment with 150 μg mL^{-1} Vd-toxins in the wild type and the *hub1-4*, *hub2-2*, and *hub1-4 hub2-2* mutants. Total RNA was extracted 24 h after the Vd-toxins treatment for RT-qPCR analysis. Seedlings

MPK3/MPK6 in the stomatal signaling pathway has been reported, and MKP1 regulates MAPK signaling specificity and cell fate decisions during stomatal development (Tamnanloo et al., 2018). H2Bub1 modulates the expression levels of *AtPTP1* and *AtMKP1* genes and affects the activation of MPK3 and MPK6 in salt-stress responses (Zhou et al., 2017).

MAPK cascades also perform roles in transcriptional reprogramming through WRKY transcription factors (Pandey and Somssich, 2009; Ishihama and Yoshioka, 2012). Some WRKY transcription factors may be regulated by MAPKs at the transcriptional and posttranscriptional levels in defense-related signaling pathways (Eulgem and Somssich, 2007; Pandey and Somssich, 2009; Ishihama and Yoshioka, 2012; Adachi et al., 2015). WRKY33 plays a vital role in Arabidopsis defenses against necrotrophic fungi (Zheng et al., 2006; Birkenbihl et al., 2012; Liu et al., 2017). WRKY33 may function as a downstream component of the MPK3/MPK6-mediated signaling pathway, and WRKY33 expression is regulated by the MPK3/MPK6 cascade (Mao et al., 2011). However, the upstream events in the MPK3/MPK6 cascade and the roles of the MPK3/MPK6-dependent signaling pathway in the regulation of defense responses to Vd-toxins are currently unknown.

Here, we show that HUB-mediated H2Bub1 plays an important role in regulating the H_2O_2-signaling pathway in defense responses to Vd-toxins. H2Bub1 regulated the expression of the NADPH oxidase *AtRbohD* and *WRKY33* by enhancing the enrichment of H3K4me3 in response to Vd-toxins. The active transcription of *WRKY33* regulates *AtRbohD* expression. In addition, H2Bub1 also affects posttranscriptional MAPK signaling. H2Bub1 is required for the activation of MPK3 and MPK6. Moreover, MPK3 and MPK6 associate with PTPs, which negatively regulated H_2O_2 production. The PTP-MPK3/6-WRKY pathway regulates H_2O_2 signals in the response against Vd-toxins in Arabidopsis.

RESULTS

HUB1 and HUB2 Are Involved in Regulating the Defense Response to Vd-Toxins

To explore the possible functions of H2Bub1 in the defense response to Vd-toxins, wild-type and HUB1 and HUB2 loss-of-function Arabidopsis plants were used in this study. First, we observed root growth after exposure to Vd-toxins in the wild type and the *hub1-4*, *hub2-2*, and *hub1-4 hub2-2* mutants of Arabidopsis. Root growth was suppressed by exposure to Vd-toxins in a concentration-dependent manner. Root lengths of the mutants were significantly shorter than those of the wild type after a 4-d Vd-toxins treatment (Fig. 1, A and B). Thus, the HUB1 and HUB2 loss-of-function Arabidopsis plants were more susceptible to Vd-toxins. We also found that Vd-toxins could induce global changes in H2Bub1 in wild-type plants (Supplemental Fig. S1).

The central features of plant defense responses are rapid cell death and the activation of defense-related genes, and this combination is known as the hypersensitive response (HR; Dangl and Jones, 2001; Greenberg and Yao, 2004). Next, we analyzed the rapid cell death and *Pathogenesis-Related Protein1* (*PR1*) gene expression after exposure to Vd-toxins in the wild type and the mutants. We used the Trypan Blue staining method to detect cell death. The extensive cell death was dramatically reduced in the leaves of the *hub1-4*, *hub2-2*, and *hub1-4 hub2-2* mutants 14 h after the Vd-toxins treatment compared with the wild type (Fig. 1, C and D). Furthermore, the relative expression levels of *PR1* were monitored by reverse transcription quantitative PCR (RT-qPCR). The expression of *PR1* was strongly increased in the wild type after the Vd-toxins treatment, whereas the expression of *PR1* was substantially reduced in the mutants, especially in the *hub1-4 hub2-2* mutant (Fig. 1E).

To corroborate that the phenotypes of the *hub* mutants resulted from the disruption of *HUB*, the *hub1-4*-complemented line *HUB1/hub1-4* was used to analyze the above phenotypes and defense responses. The phenotype of the *HUB1/hub1-4* complementation line was restored to that of the wild type (Fig. 1).

Thus, the mutants showed the suppression of root growth, reduction of Vd-toxins-induced cell death, and expression of defense genes, suggesting that HUB1 and HUB2 play important roles in regulating defense responses to Vd-toxins in Arabidopsis.

HUB1 and HUB2 Loss-of-Function Plants Have Reduced Vd-Toxins-Induced H_2O_2 Production Levels

Following successful pathogen recognition, ROS are proposed to orchestrate the establishment of plant defenses (Torres et al., 2006). H_2O_2 accumulation is a marker of the cellular defense response (Sang and

Figure 3. (*Continued.*)
treated with double distilled water were used as controls. Error bars indicate SD; $n = 3$. E, Schematic diagram of the *AtRbohD* and *AtRbohF* genes. *AtRbohD* P1, *AtRbohD* P2, and *AtRbohF* P1 are gene body regions; arrows indicate transcription start sites. F and G, Relative enrichments of H2Bub1 and H3K4me3 in the *AtRbohD* locus after treatment with Vd-toxins in the wild type and the *hub1-4*, *hub2-2*, and *hub1-4 hub2-2* mutants. Chromatin was extracted 12 h after the Vd-toxins treatment, and immunoprecipitated DNA was analyzed using qPCR. Data were determined as percentages of H2Bub1/H3 and H3K4me3/H3 for each individual gene position. Relative enrichments of H2Bub1 and H3K4me3 in the *AtRbohF* P1 locus were used as negative controls. Error bars indicate SD; $n = 3$. Different letters represent significant differences at $P < 0.05$ by one-way ANOVA with Tukey's honestly significant difference posthoc tests. All experiments were repeated three times.

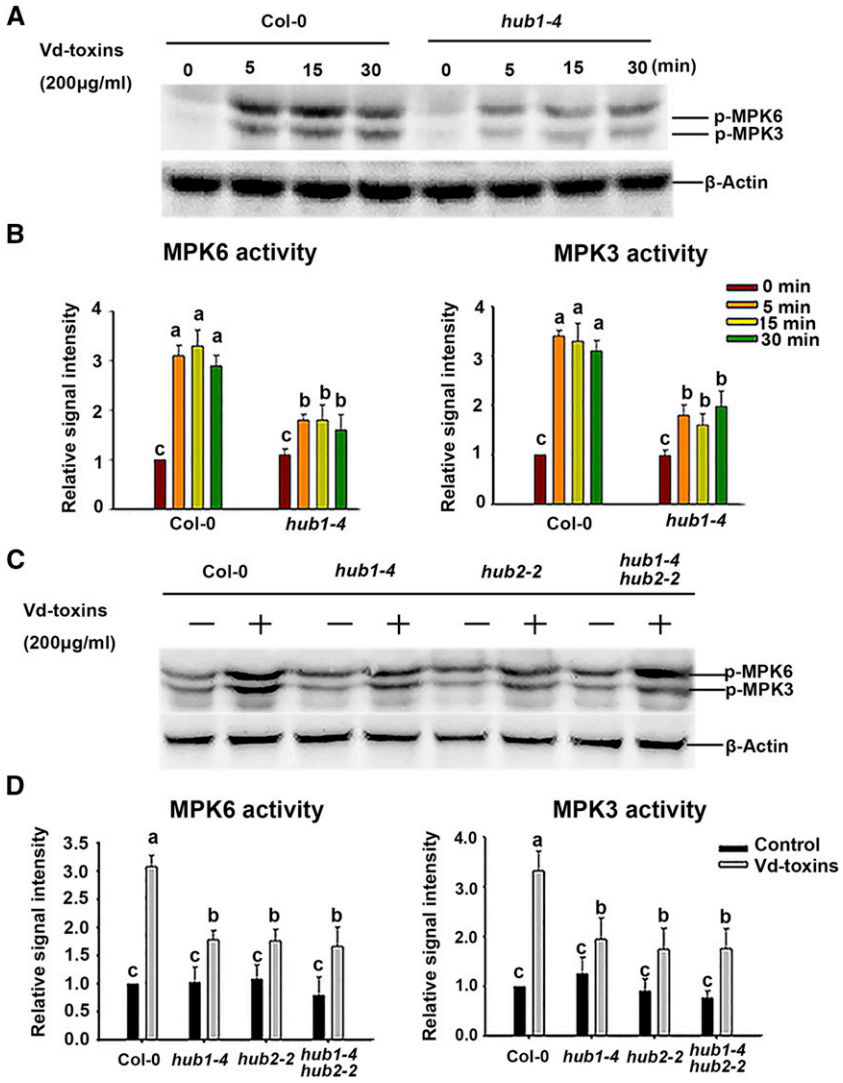

Figure 4. HUB1 and HUB2 affect the activation of MPK3 and MPK6 in response to the Vd-toxins treatment in Arabidopsis. A, The kinase activities of MPK3 and MPK6 were detected by immunoblotting using anti-phospho-p44/42 MAPK antibodies (p-MPK6 and p-MPK3). Seedlings (7 d old) of wild-type Columbia-0 (Col-0) and the *hub1-4* mutant were treated with 200 μg mL^{-1} Vd-toxins, and then total proteins were extracted after various times for immunoblot analysis. β-Actin was used as the loading control. Results are presented three independent biological replicates. B, Quantification of the kinase activities of MPK3 and MPK6 in A using ImageJ software. Error bars indicate SD; $n = 3$. C, The kinase activities of MPK3 and MPK6 were measured in the wild type and the *hub1-4*, *hub2-2*, and *hub1-4 hub2-2* mutants. Seedlings (7 d old) of the wild type and mutants were treated with 200 μg mL^{-1} Vd-toxins, and then total proteins were extracted after 30 min for immunoblot analysis. Results are presented three independent biological replicates. D, Quantification of the kinase activities of MPK3 and MPK6 in C using ImageJ software. Error bars indicate SD; $n = 3$. Different letters represent significant differences at $P < 0.05$ by one-way ANOVA with Tukey's honestly significant difference posthoc tests.

Macho, 2017). We next explored whether HUB1 and HUB2 are involved in regulating H_2O_2 production in defense responses to Vd-toxins. H_2O_2 in Arabidopsis leaves was labeled using a 2′,7′-dichlorofluorescein diacetate (H_2DCF-DA) fluorescent probe. The fluorescence intensity observed in the wild type substantially increased after the Vd-toxins treatment, whereas the fluorescence intensity was only slightly increased in *hub1-4*, *hub2-2*, and *hub1-4 hub2-2* mutants. The intensity of the *HUB1/hub1-4* complementation line was similar to that of the wild type (Fig. 2, A and B). Furthermore, we measured the H_2O_2 content in leaves using a chromogenic peroxidase-coupled assay, and, similar to the above result, the level of H_2O_2 accumulation induced by the Vd-toxins was dramatically reduced in the mutant compared with the wild type (Fig. 2C).

The *Glutathione-S-Transferase1* (*GST1*) gene can function as a marker gene for ROS (Love et al., 2005). To determine whether HUB1 and HUB2 loss-of-function plants affect H_2O_2 production at the transcriptional level, we measured the relative expression levels of *GST1* using RT-qPCR. The expression of *GST1* was strongly increased in the wild type after the Vd-toxins treatment, whereas the expression of *GST1* was substantially reduced in the mutants. The expression level in the *HUB1/hub1-4* complementation line was partially restored to that of the wild type (Fig. 2D). Thus, HUB1 and HUB2 play functional roles in regulating H_2O_2 production in Arabidopsis defense responses to Vd-toxins.

HUB1 and HUB2 Regulate NADPH Oxidase *AtRbohD* Expression

NADPH oxidases are necessary for the H_2O_2 production induced by Vd-toxins in Arabidopsis (Yao et al., 2011). To further dissect the effect of H2Bub1 on H_2O_2 production, we first examined H_2O_2 production induced by Vd-toxins in the wild type, the NADPH oxidase loss-of-function mutants *atrbohD* and *atrbohF*,

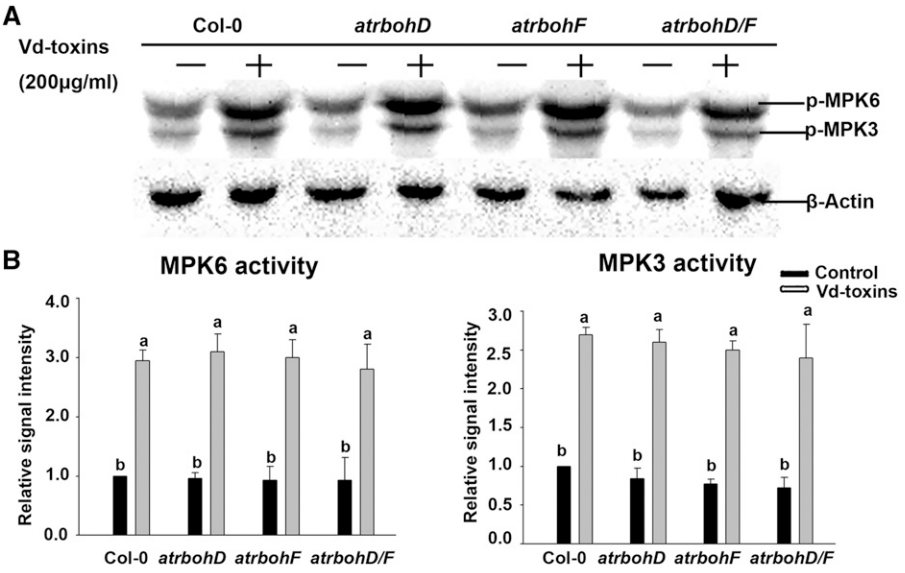

Figure 5. Activation states of MPK3 and MPK6 induced by Vd-toxins in wild-type Arabidopsis Columbia-0 (Col-0) and *atrbohD*, *atrbohF*, and *atrbohD/F* mutants. A, The kinase activities of MPK3 and MPK6 were measured in the wild type and the *atrbohD*, *atrbohF*, and *atrbohD/F* mutants. Seedlings (7 d old) of the wild type and mutants were treated with 200 μg mL^{-1} Vd-toxins, and total proteins were then extracted after 30 min for immunoblot analysis. β-Actin was used as the loading control. Results are presented three independent biological replicates. B, Quantification of the kinase activities of MPK3 and MPK6 in A using ImageJ software. Error bars indicate SD; $n = 3$. Different letters represent significant differences at $P < 0.05$ by one-way ANOVA with Tukey's honestly significant difference posthoc tests.

as well as the *atrbohD/F* double mutant, using the H_2DCF-DA staining assay. H_2O_2 production was induced by Vd-toxins, and the H_2O_2 level displayed a time-dependent increase in both the wild type and mutants. However, H_2O_2 production was significantly lower in *atrbohD*, *atrbohF*, and *atrbohD/F* than in the wild type (Fig. 3, A and B). Interestingly, H_2O_2 production was significantly greater in the *atrbohF* mutant, especially later in the treatment (25–30 min), than in the *atrbohD* or *atrbohD/F* mutant.

Next, we examined the expression levels of *AtRbohD* and *AtRbohF* in the wild type and the *hub1-4*, *hub2-2*, and *hub1-4 hub2-2* mutants after Vd-toxins treatment. The expression of *AtRbohD* was significantly up-regulated in the wild type, whereas it was slightly up-regulated in *hub1-4*, *hub2-2*, and *hub1-4 hub2-2* mutants. In contrast, no marked differences in the expression levels of *AtRbohF* were detected between the *hub1-4*, *hub2-2*, and *hub1-4 hub2-2* mutants and the wild type (Fig. 3, C and D).

To further investigate how HUB1 and HUB2 influenced the transcription of *AtRbohD*, we performed a chromatin immunoprecipitation (ChIP) assay using an anti-H2Bub1 antibody against chromatin derived from the wild type and the *hub1-4*, *hub2-2*, and *hub1-4 hub2-2* mutants, and we designed two fragments based on the chromatin of *AtRbohD* for ChIP-qPCR, *AtRbohD* P1 (193–370) and *AtRbohD* P2 (724–901; Fig. 3E). qPCR was performed to detect the relative H2Bub1 enrichment in the chromatin of *AtRbohD*, while the relative H2Bub1 enrichment in the chromatin of *AtRbohF* P1 (406–583) was used as the negative control. H2Bub1 was enriched intensively in the chromatin of the *AtRbohD* locus of the wild type, whereas it was enriched weakly in the *hub* mutants. Moreover, H2Bub1 was obviously increased in the chromatin of *AtRbohD* of the wild type after the Vd-toxins treatment, while it was barely increased in the *hub* mutants (Fig. 3F).

In general, histone H3K4me3 is necessary for gene activation while H3K27me is associated with transcriptional repression (Li et al., 2007). H2Bub1 is required for H3K4 and H3K79 methylation in yeast (Lee et al., 2007). Therefore, we performed ChIP assays using an anti-H3K4me3 antibody to detect the level of H3K4me3 enrichment in the chromatin of *AtRbohD*. H3K4me3 was increased in the chromatin of *AtRbohD* after Vd-toxins treatment in both the wild type and *hub* mutants; however, it was lower in the *hub* mutants (Fig. 3G). These results indicated that H2Bub1 regulated the expression of *AtRbohD* by enhancing the level of H3K4me3 in the *AtRbohD* locus after the Vd-toxins treatment.

Thus, *AtRbohD* may play a more important role than *AtRbohF* in H_2O_2 production induced by Vd-toxins. Additionally, H2Bub1 regulates the expression of the NADPH oxidase *AtRbohD*, which is associated with the enhancement of H3K4me3 in the chromatin of *AtRbohD*.

HUB1 and HUB2 Are Required for the Activation of MPK3 and MPK6 during Defense Responses to Vd-Toxins

MPK3 and MPK6 have emerged as central players in MAPK-mediated stress signaling (Bartels et al., 2009; Pitzschke, 2015), while H2Bub1 is required for the activation of MPK3 and MPK6 in modulating salt-stress tolerance in Arabidopsis (Zhou et al., 2017). Therefore, we examined whether MAPK is involved in the Vd-toxins-induced responses and whether HUB1 and HUB2 are required for the activation of MPK3 and MPK6 during defense responses. To investigate the latter, we confirmed the activation of MPK3 and MPK6 in wild-type and mutant seedlings. Seedlings of the 7-d-old wild type and the *hub1-4* mutant were

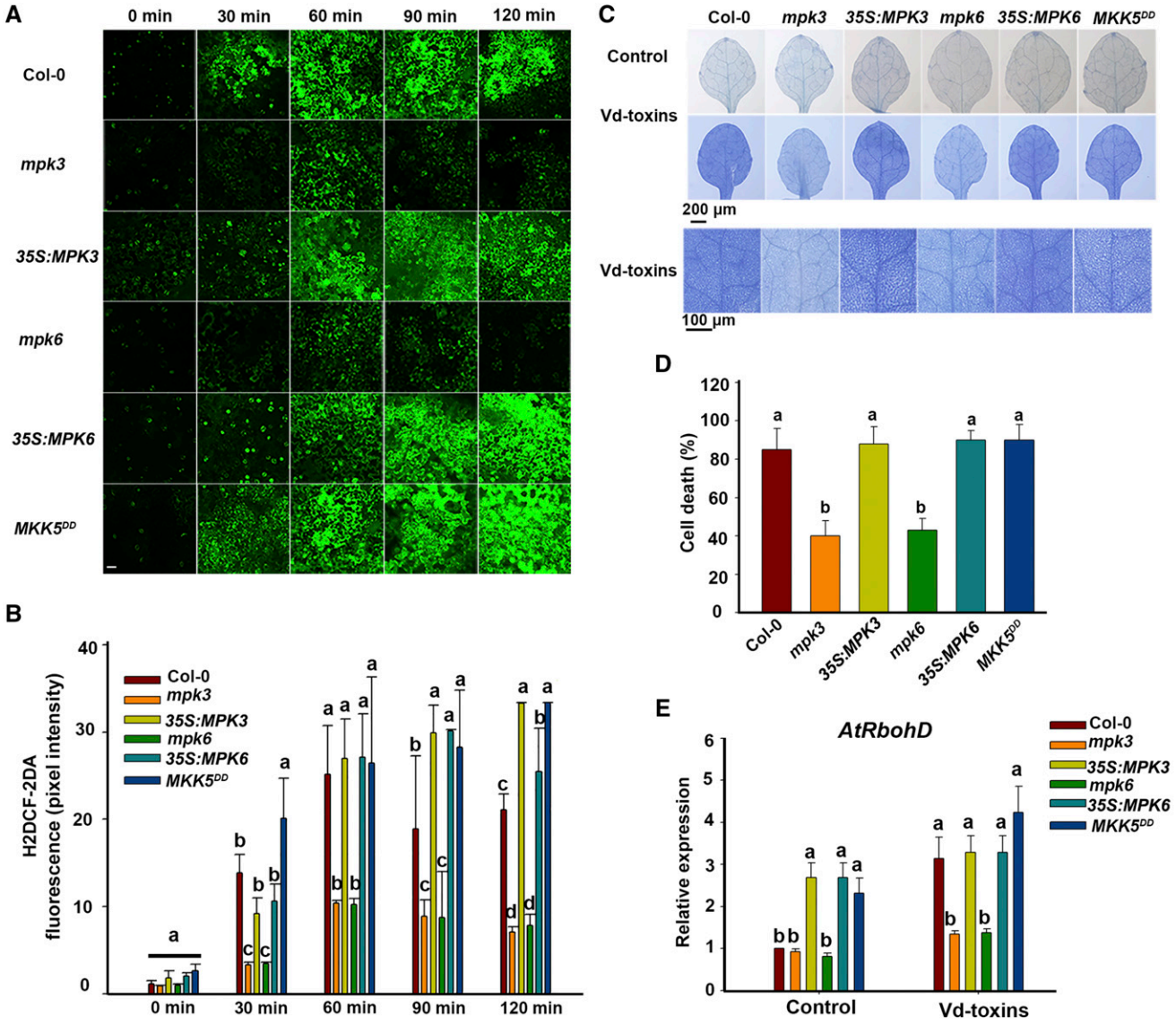

Figure 6. MPK3 and MPK6 regulate H_2O_2 production and *RbohD* expression in Arabidopsis. A, H_2O_2 was detected in the leaves of wild-type Columbia-0 (Col-0), the *mpk3* and *mpk6* mutants, the *35S:MPK3* and *35S:MPK6* lines, and the *MKK5*^{DD} mutant using fluorescence resulting from H_2DCF-DA, as described in "Materials and Methods." Leaves were treated with Vd-toxins plus 15 μM DEX. Bar = 20 μm. B, Quantification of the H_2DCF-DA fluorescence intensities in A. Error bars indicate SD; $n = 8$. C, Cell death in cotyledons of wild-type, the *mpk3* and *mpk6* mutants, the *35S:MPK3* and *35S:MPK6* lines, and *MKK5*^{DD} Arabidopsis seedlings. Cotyledons of 14-d-old seedlings were treated 14 h with 150 μg mL^{-1} Vd-toxins plus 15 μM DEX and stained with Trypan Blue. Seedlings treated with 15 μM DEX were used as controls. D, Quantification of the cell death rates induced by Vd-toxins in C using ImageJ software. Error bars indicate SD; $n = 15$. E, Relative expression levels of *AtRbohD* after treatment in wild-type, the *mpk3* and *mpk6* mutants, the *35S:MPK3* and *35S:MPK6* lines, and *MKK5*^{DD} seedlings. Total RNA was extracted 12 h after the Vd-toxins treatment for RT-qPCR analysis. Error bars indicate SD; $n = 9$. Different letters represent significant differences at $P < 0.05$ by one-way ANOVA with Tukey's honestly significant difference posthoc tests. All experiments were repeated three times.

independently treated with 200 μg mL^{-1} Vd-toxins, and samples were taken at various times. MPK3 and MPK6 were rapidly activated, and activities were significantly elevated in the wild type within 30 min, whereas their activity levels were partially elevated in the *hub1-4* mutant compared with the wild type (Fig. 4, A and B; Supplemental Fig. S2). Furthermore, seedlings of *hub2-2* and *hub1-4 hub2-2* mutants were also independently treated with 200 μg mL^{-1} Vd-toxins for 30 min, and the results were consistent with those of the *hub1-4* mutant (Fig. 4, C and D). Thus, HUB1 and HUB2 appear to be required for the activation of MPK3 and MPK6 during defense responses to Vd-toxins.

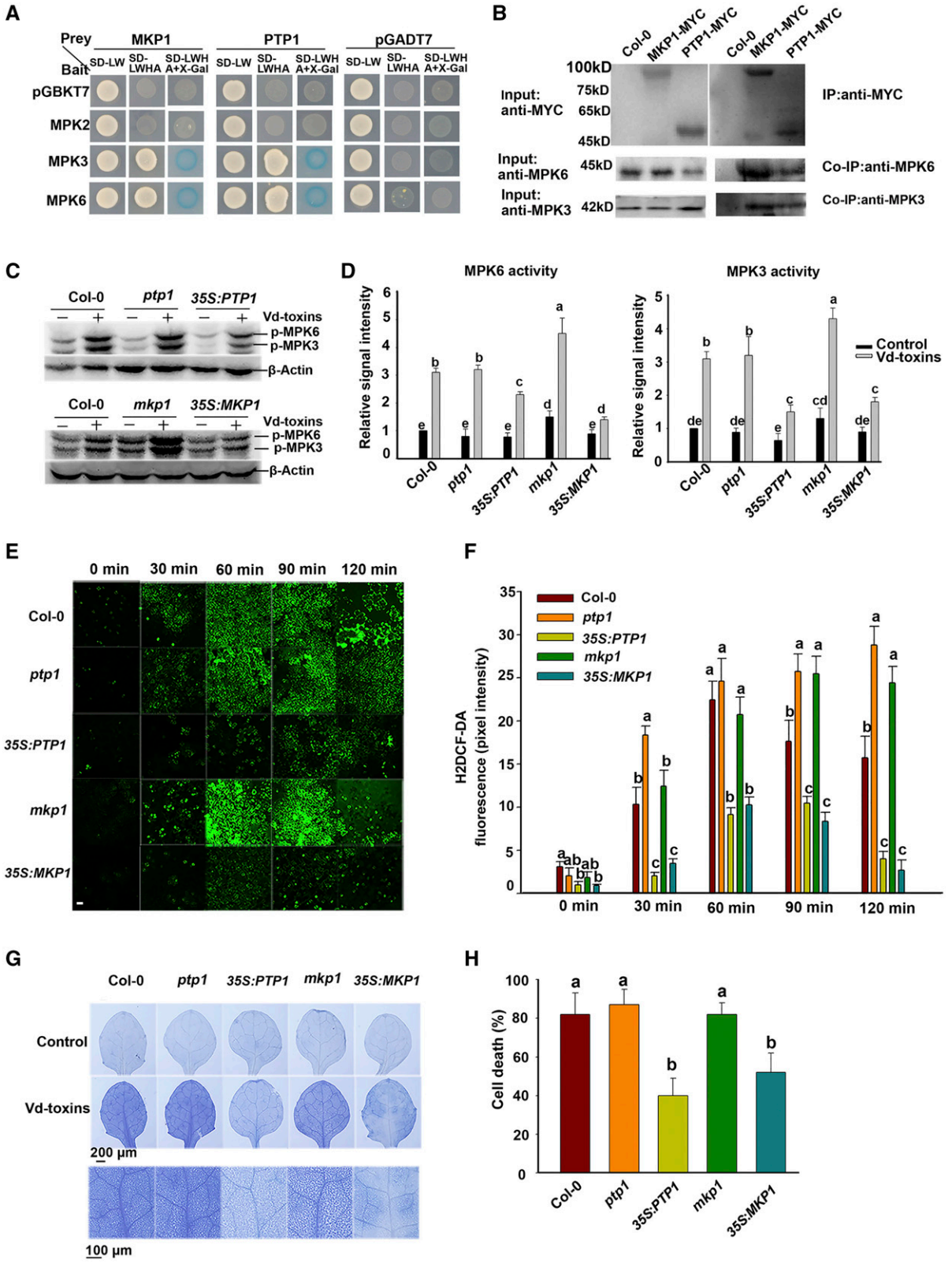

Figure 7. MPK3 and MPK6 interact with PTP1 and MKP1, which negatively regulate H_2O_2 production in Arabidopsis. A, Interactions of PTP1 and MKP1 with MPK3 and MPK6 in the yeast two-hybrid system. The experiments were performed three times with similar results. B, Co-IP of MPK3 and MPK6 interactions with PTP1 and MKP1. Total proteins were extracted from 15-d-old wild-type Columbia-0 (Col-0) and transgenic *35S:PTP1* and *35S:MKP1* lines. Input and immunoprecipitated proteins were

MPK3 and MPK6 Are Involved in Regulating *AtRbohD*-Mediated H_2O_2 Production

To determine whether H_2O_2 production affected the activation of MPK3 and MPK6 in response to Vd-toxins or whether the activation of MPK3 and MPK6 affected the H_2O_2 production induced by Vd-toxins, we examined the activation of MPK3/MPK6 and H_2O_2 production in the wild type, *atrbohD*, *atrbohF*, *atrbohD/F*, *mpk3*, and *mpk6* mutants, the *35S:MPK3* and *35S:MPK6* lines, and $MKK5^{DD}$, a constitutively active MKK5 kinase mutant, which leads to the rapid activation of MPK3 and MPK6 during dexamethasone (DEX) treatment.

We first examined the activation of MPK3 and MPK6 after the Vd-toxins treatment in the wild type and the *atrbohD*, *atrbohF*, and *atrbohD/F* mutants. The activation states of MPK3 and MPK6 were induced by Vd-toxins in the mutants and the wild type; however, there were no significant differences in the activation levels of MPK3 and MPK6 among the tested lines (Fig. 5). H_2O_2 production was significantly lower in *atrbohD*, *atrbohF*, and *atrbohD/F* mutants compared with the wild type (Fig. 3, A and B). Thus, the activation states of MPK3 and MPK6 are not affected by H_2O_2 production triggered by Vd-toxins.

To further determine whether MPK3 and MPK6 affected H_2O_2 production induced by Vd-toxins, we examined H_2O_2 production in the wild type, the *mpk3* and *mpk6* mutants, the *35S:MPK3* and *35S:MPK6* lines, and $MKK5^{DD}$. H_2O_2 production increased dramatically after the Vd-toxins treatment in the wild type, *35S:MPK3*, *35S:MPK6*, and $MKK5^{DD}$, whereas the induced H_2O_2 production was significantly reduced in the *mpk3* and *mpk6* mutants compared with the wild type (Fig. 6, A and B). Trypan Blue staining was used to determine whether the *mpk3* and *mpk6* mutations affected the HR cell death-related phenotypes. As shown in Figure 6, C and D, the *mpk3* and *mpk6* mutations reduced the extensive cell death, indicating that MPK3 and MPK6 are associated with HR-related cell death in response to Vd-toxins. Furthermore, we examined the expression of *AtRbohD* in the wild type, the *mpk3* and *mpk6* mutants, the *35S:MPK3* and *35S:MPK6* lines, and $MKK5^{DD}$ after exposure to Vd-toxins. As shown in Figure 6E, the expression levels of *AtRbohD* in *mpk3* and *mpk6* mutants were much lower than those in the wild type, *35S:MPK3* and *35S:MPK6* lines, and $MKK5^{DD}$, indicating that the expression of *AtRbohD* is positively regulated by MPK3 and MPK6. Thus, MPK3 and MPK6 putatively regulate H_2O_2 production, and MPK3 and MPK6 are involved in regulating the expression of *RbohD* during the defense response to Vd-toxins.

MPK3 and MPK6 Interact with PTP1 and MKP1, and PTP1 and MKP1 Negatively Regulate H_2O_2 Production

PTP1 and MKP1 are important regulators of MPK3/MPK6-dependent stress signaling (Bartels et al., 2009). To examine whether PTP1 and MKP1 affect MPK3 and MPK6 signaling involved in the defense response to Vd-toxins, we used yeast two-hybrid and coimmunoprecipitation (Co-IP) assays to detect whether PTP1 or MKP1 interacts with MPK3 or MPK6. PTP1 and MKP1 interacted with MPK3 and MPK6 (Fig. 7, A and B). To further determine whether PTP1 and MKP1 affected the activation states of MPK3 and MPK6, kinase activity assays were performed by immunoblotting using an anti-phospho-p44/42 antibody. The wild-type plants were independently transformed with vectors expressing *PTP1* and *MKP1* cDNA driven by the strong 35S promoter of *Cauliflower mosaic virus* (*35S:PTP1* and *35S:MKP1*). The MPK3 and MPK6 activity levels were significantly elevated by exposure to Vd-toxins in the wild type and the *ptp1* and *mkp1* mutants, whereas the MPK3 and MPK6 activity levels were partially increased in the *35S:PTP1* and *35S:MKP1* lines (Fig. 7, C and D). Thus, PTP1 and MKP1 act as negative regulators of MPK3 and MPK6 activities.

To further investigate whether PTP1 and MKP1 affect H_2O_2 production, we examined H_2O_2 production induced by Vd-toxins in the wild type, the *ptp1* and *mkp1* mutants, and the *35S:PTP1* and *35S:MKP1* lines. The H_2O_2 production levels were significantly increased by the Vd-toxins treatment in *ptp1* and *mkp1* mutants compared with the wild type, whereas H_2O_2 production levels were markedly decreased in *35S:PTP1* and

Figure 7. (*Continued.*)
analyzed by independently immunoblotting with anti-MYC, anti-MPK3, and anti-MPK6 antibodies. C, The kinase activities of MPK3 and MPK6 were detected by immunoblotting using anti-phospho-p44/42 MAPK antibodies (p-MPK6 and p-MPK3). Seedlings (7 d old) of the wild type, the *ptp1* and *mkp1* mutants, and the *35S:PTP1* and *35S:MKP1* lines were treated with 200 μg mL^{-1} Vd-toxins, and the total proteins were then extracted at various times for immunoblot analysis. β-Actin was used as the loading control. D, Quantification of the kinase activity levels of MPK3 and MPK6 in C using ImageJ software. Results are presented three independent biological replicates. Error bars indicate SD; $n = 3$. E, H_2O_2 was detected in the leaves of the wild type, the *ptp1* and *mkp1* mutants, and the *35S:PTP1* and *35S:MKP1* lines using a fluorescence assay with H_2DCF-DA, as described in "Materials and Methods." Bar = 20 μm. F, Quantification of the H_2DCF-DA fluorescence intensities in E. Error bars indicate SD; $n = 8$. G, Cell death induced by Vd-toxins in cotyledons of the wild type, the *ptp1* and *mkp1* mutants, and the *35S:PTP1* and *35S:MKP1* lines. Cotyledons of 14-d-old seedlings were treated 14 h with 150 μg mL^{-1} Vd-toxins and stained with Trypan Blue. H, Quantification of the cell death rates induced by Vd-toxins in G using ImageJ software. Error bars indicate SD; $n = 9$. Different letters represent significant differences at $P < 0.05$ by one-way ANOVA with Tukey's honestly significant difference posthoc tests. All experiments were repeated three times.

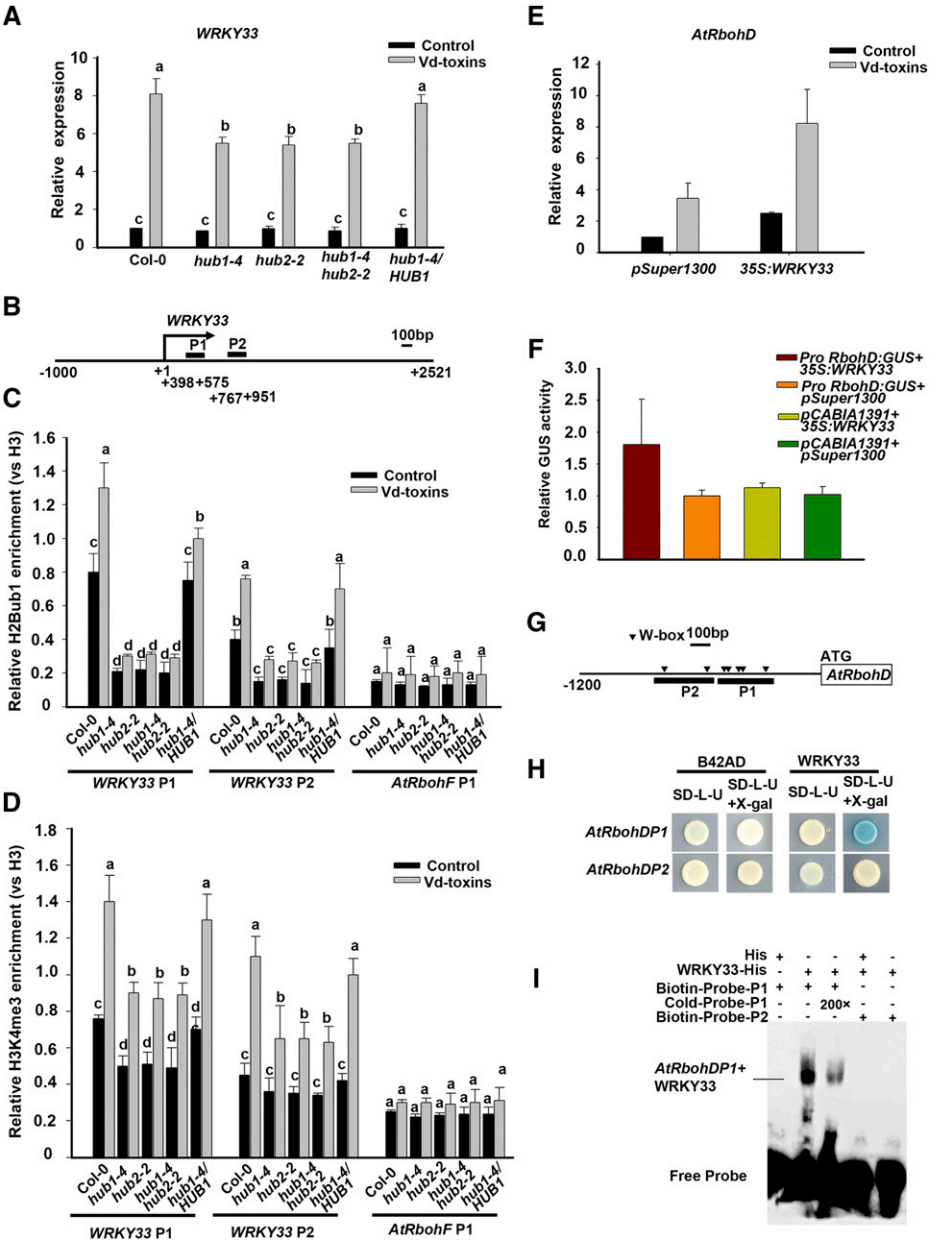

Figure 8. HUB1 and HUB2 regulated the expression of *WRKY33* in response to Vd-toxins, and WRKY33 regulated the expression of *AtRbohD* in Arabidopsis. A, The relative expression levels of *WRKY33* induced by 150 μg mL^{-1} Vd-toxins in wild-type Columbia-0 (Col-0), the *hub1-4*, *hub2-2*, and *hub1-4 hub2-2* mutants, and the *HUB1/hub1-4* complementation line. Error bars indicate SD. B, Schematic diagram of the *WRKY33* gene. P1 and P2 are gene body regions; the arrow indicates the transcription start site. C and D, Relative enrichments of H2Bub1 and H3K4me3 in the *WRKY33* locus after treatment with 150 μg mL^{-1} Vd-toxins in the wild type, the *hub1-4*, *hub2-2*, and *hub1-4 hub2-2* mutants, and the *HUB1/hub1-4* complementation line. Chromatin was extracted 12 h after the Vd-toxins treatment, and immunoprecipitated DNA was analyzed by qPCR. Data were determined as the percentages of H2Bub1/H3 and H3K4me3/H3 for each individual gene position. Relative enrichments of H2Bub1 and H3K4me3 in the *AtRbohF* P1 locus were used as negative controls. Error bars indicate SD. Different letters in A, C, and D represent significant differences at $P < 0.05$ by one-way ANOVA with Tukey's honestly significant difference posthoc tests. E, WRKY33 regulates the expression of *AtRbohD*. The protoplasts of Arabidopsis harboring *35S:WRKY33* were used. The expression of *AtRbohD* was examined after the protoplasts were exposed to Vd-toxins for 4 h. *pSuper1300* was used as the negative control. Error bars indicate SD. F, GUS activity measurement in *N. benthamiana* leaves after the transient expression of *ProRbohD:GUS* and *35S:WRKY33*. *pCAMBIA1391* and *pSuper1300* were used as negative controls. LUC was used as an internal control. G, Schematic diagram showing the promoter structure of the *AtRbohD* gene. The upstream regions and part of the coding region are indicated by black wide lines and a white box, respectively. The solid arrowheads indicate the sites containing W-boxes in the *AtRbohD* promoter. The two fragments (P1 and P2) used for the yeast one-hybrid assay and EMSA are indicated. H, Yeast

35S:MKP1 lines (Fig. 7, E and F). Moreover, we examined whether PTP1 and MKP1 affected the defense response to Vd-toxins. Trypan Blue staining indicated that the *35S:PTP1* and *35S:MKP1* lines reduced the extensive cell death (Fig. 7, G and H). Thus, PTP1 and MKP1 act as negative regulators of defense responses to Vd-toxins. These data suggest that PTP1 and MKP1 negatively regulated H_2O_2 production and inhibited the activity levels of MPK3 and MPK6 during defense responses to Vd-toxins.

HUB1 and HUB2 Regulate *WRKY33* Expression and WRKY33 Regulates *AtRbohD* Expression

WRKY33 is a pathogen-inducible transcription factor, and its expression is regulated by the MPK3/MPK6 cascade (Mao et al., 2011). Therefore, we hypothesized that HUB1 and HUB2 are involved in regulating the expression of *WRKY33* in response to Vd-toxins. To determine whether HUB1 and HUB2 loss-of-function plants affected *WRKY33* expression, the relative expression levels of *WRKY33* were analyzed after exposure to Vd-toxins in the wild type, the *hub1-4*, *hub2-2*, and *hub1-4 hub2-2* mutants, and the *HUB1/hub1-4* complementation line using RT-qPCR. The expression of *WRKY33* was strongly up-regulated in the wild type, while it was reduced in the mutants compared with the wild type. The expression level in the *HUB1/hub1-4* complementation line was restored to that of the wild type (Fig. 8A). ChIP assays were performed to examine the levels of H2Bub1and H3K4me3 enrichment in the chromatin of *WRKY33* in the wild type, the *hub1-4*, *hub2-2*, and *hub1-4 hub2-2* mutants, and the *HUB1/hub1-4* complementation line. Two fragments on the chromatin of *WRKY33* were targeted for ChIP-qPCR (Fig. 8B). H2Bub1 enrichment was strongly detected in the chromatin of *WRKY33* in the wild type, but only a weak enrichment was detected in the *hub* mutants. H2Bub1 was obviously increased in the chromatin of *WRKY33* of the wild type after the Vd-toxins treatment, while it was only slightly increased in the *hub* mutants (Fig. 8C). Moreover, the level of H3K4me3 was greater in the chromatin of *WRKY33* after Vd-toxins treatment in the wild type than in the *hub* mutant (Fig. 8D). These results suggested that HUB1 and HUB2 regulated the expression of *WRKY33* by enhancing the enrichment of H3K4me3 after Vd-toxins treatment.

Next, we determined whether WRKY33 regulated the expression of the *AtRbohD* gene. We detected the gene expression of *AtRbohD* in a *WRKY33* overexpression line. The protoplasts of Arabidopsis harboring *35S:WRKY33* were used. *AtRbohD* was up-regulated in the *35S:WRKY33* line compared with the control, which was protoplasts harboring the empty vector (Fig. 8E).

To further substantiate the role of WRKY33 in the regulation of *AtRbohD* expression, we performed transient transactivation assays in *Nicotiana benthamiana* leaves to determine whether WRKY33 regulates the

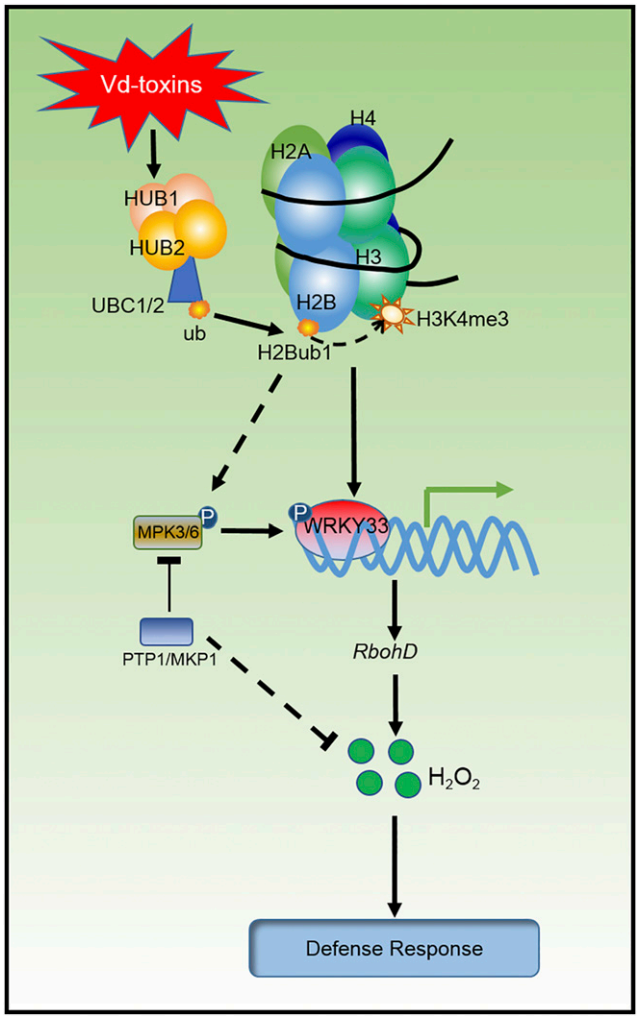

Figure 9. Model of the H2Bub1 mechanism used to regulate defense responses to Vd-toxins in Arabidopsis. In this model, HUB-mediated H2Bub1 regulates the expression of the NADPH oxidase *RbohD* and *WRKY33* by enhancing the enrichment of H3K4me3 in response to Vd-toxins. H2Bub1 also affects posttranscriptional MAPK signaling. H2Bub1 is required for the activation of MPK3 and MPK6. Phosphorylation of WRKY33 by MPK3 and MPK6 regulates the expression of *RbohD*. Moreover, MPK3 and MPK6 associate with PTPs, which negatively regulate H_2O_2 production. The PTP-MPK3/6-WRKY pathway regulates H_2O_2 signals in the responses against Vd-toxins in Arabidopsis.

Figure 8. (*Continued.*)
one-hybrid assay showing that WRKY33 binds to the *AtRbohD* promoter. I, EMSA showing WRKY33 binding to the *AtRbohD* promoter. Biotin-labeled fragments of the *AtRbohD* promoter that contained W-boxes were used as probes. Each experiment was repeated three times with similar results.

expression of *AtRbohD*. The leaves were inoculated with *Agrobacterium tumefaciens* containing *ProRbohD:GUS* and *35S:WRKY33*. *pCAMBIA1391* and *pSuper1300* were used as negative controls. Luciferase (LUC) was used as the loading control. The expression of *AtRbohD* was greater in leaves that were cotransformed with *35S:WRKY33* than in the control (Fig. 8F). Next, we performed yeast one-hybrid assays and electrophoresis mobility shift assays (EMSAs) to determine whether WRKY33 bound directly to the promoter of *AtRbohD*. We analyzed the sequences of *AtRbohD* promoter regions and found that the P1 and P2 fragments of the *AtRbohD* promoter contain W-box structures (Fig. 8G). The P1 and P2 fragments were independently inserted into the pLacZi2μ vector, and the coding sequence of *WRKY33* was inserted into the pB42AD vector. Only the strain carrying both the AD-WRKY33 and *AtRbohD P1:LacZ* plasmids turned blue, indicating an interaction (Fig. 8H).

To perform the EMSA, the recombinant WRKY33 fused with a His tag (WRKY33-His) was purified from a prokaryotic system. The P1 and P2 fragments of the *AtRbohD* promoter were each labeled with biotin. WRKY33-His could bind to the *AtRbohD* P1, while no binding was observed between the P2 fragment and the WRKY33-His. The negative control and the addition of the competitive probe (Cold-Probe-P1) also resulted in no binding and weak binding, respectively (Fig. 8I).

Thus, HUB1 and HUB2 regulate the expression of *WRKY33* by enhancing the enrichment of H3K4me3 in response to Vd-toxins. WRKY33 directly binds to *AtRbohD* promoter and functions as a transcription factor to regulate the expression of *AtRbohD*.

DISCUSSION

In this study, we demonstrated that HUB-mediated H2Bub1 plays an important role in regulating the H_2O_2 signaling pathway in the defense response to Vd-toxins. H2Bub1 regulated the expression of the NADPH oxidase *AtRbohD* and *WRKY33* genes. H2Bub1 also affects posttranscriptional MAPK signaling. H2Bub1 is required for the activation of MPK3 and MPK6. Moreover, MPK3 and MPK6 associate with PTPs to affect H_2O_2 signal accumulation. The WRKY33 transcription factor is necessary for regulating *AtRbohD*'s expression. Thus, we have increased our knowledge of the molecular regulatory mechanisms of H2Bub1 that are involved in the defense response against Vd-toxins.

H_2O_2 signals induce large transcriptional changes and cellular reprogramming to control a large array of biological processes, ranging from the regulation of growth and development to responses to biotic and abiotic stimuli (Gadjev et al., 2006; Mittler et al., 2011). NADPH oxidase has a pivotal role in H_2O_2 production under biotic and abiotic stress conditions (Suzuki et al., 2011). In Arabidopsis, there are 10 different *Rboh* genes and their expression is mainly transcriptionally controlled in a tissue-specific manner. The *RbohD* and *RbohF* genes belong to the group expressed throughout the whole plant, and *RbohD* and *RbohF* are capable of generating H_2O_2 in response to pathogen attacks (Torres et al., 2002; Torres and Dangl, 2005). However, the expression levels of *AtRbohD* and *AtRbohF* are differentially modulated by pathogen-associated molecular patterns, and this could account for their action specificities (Morales et al., 2016). In this study, we found that *AtRbohD* plays a more important role than *AtRbohF* in the H_2O_2 accumulation induced by Vd-toxins. Moreover, HUB1 and HUB2 are involved in regulating the expression of *AtRbohD*.

H2Bub1 controls flowering time primarily through the transcriptional activation of *FLC*, and H2Bub1 is required for the enhancement of H3K4me3 in the chromatin of *FLC* and other *FLC* clade genes in Arabidopsis (Cao et al., 2008). H2Bub1 also regulates the expression levels of circadian clock genes (e.g. *CCA1* and *TOC1*) by increasing the H3K4me3 deposition in their chromatin (Himanen et al., 2012; Malapeira et al., 2012). However, H2Bub1 and H3K4me3 deposition were only connected at some gene-specific chromatin regions. SET DOMAIN GROUP8 (SDG8; which encodes a histone methyl transferase) and SDG25 affect distinct H3K4 and H3K36 methylations and regulate the expression of plant immunity genes directly through histone Lys methylation or indirectly through H2Bub1 (Lee et al., 2016). In addition, SA2Lb (a euchromatic protein that functionally associates with an AtCOMPASS-like complex) mediates H3K4me3 deposition independent of H2Bub1 (Fiorucci et al., 2019). The interaction between H2Bub1 and H3K4me3 deposition in plant defense responses is poorly understood. Our results showed that HUB1 and HUB2 regulate the expression of *AtRbohD* by enhancing the level of H3K4me3 in the chromatin of *AtRbohD*. Therefore, we concluded that *AtRbohD* is responsible for H_2O_2 accumulation during responses to Vd-toxins in Arabidopsis and that H2Bub1 regulates the expression of *AtRbohD*, which is associated with H3K4me3.

MAPK activation may lead to ROS production, and MPK3/MPK6 may regulate the ROS bursts from NADPH oxidases (Zhang et al., 2007; Asai et al., 2008). Conversely, MAPKs may function downstream of ROS bursts when triggering plant immunity (Apel and Hirt, 2004; Pitzschke and Hirt, 2009). In this study, we demonstrated that MPK3 and MPK6 act as positive regulators of defense responses to Vd-toxins. Additionally, MPK3/MPK6 played important roles upstream of H_2O_2 accumulation, and they regulated the *AtRbohD*-dependent H_2O_2 production in the defense response to Vd-toxins. The results indicate that *AtRbohD*-dependent H_2O_2 production is required for the activation of MPK3 and MPK6 after exposure to Vd-toxins. Thus, MAPK activation occurs upstream of H_2O_2 production in this pathway. This is consistent with an earlier study (Zhang et al., 2007). Thus, the mechanisms of MAPK-controlled H_2O_2 production and H_2O_2-controlled MAPK activity should be discerned in the near future.

Protein Tyr phosphorylation plays an important role in the regulation of MAPK signaling (Tena et al., 2001; Zhang and Klessig 2001; Ghelis et al., 2008; Nemoto et al., 2015). The two main Tyr phosphatases that dephosphorylate activated MAPKs are MKP1 and PTP1 (Bartels et al., 2009). For example, PTP1 and MKP1 act as repressors of MPK3/MPK6-dependent stress signaling (Bartels et al., 2009), and MKP1 acts as a negative regulator of MPK6-mediated pathogen-associated molecular pattern responses and resistance against bacteria (Anderson et al., 2011). Therefore, it is likely that PTP1 and MKP1 have negative functions in defense signaling pathways. In this study, we demonstrated that PTP1 and MKP1 interact with MPK3 and MPK6 and negatively regulate H_2O_2 production. A previous study showed that H2Bub1 modulates the expression levels of *AtPTP1* and *AtMKP1* genes and affects the activation states of MPK3 and MPK6 in salt-stress responses (Zhou et al., 2017).

WRKY transcription factors are transcriptional regulators of signaling pathways involved in biotic and abiotic stress responses, and they act by specifically binding to W-boxes (TTGACC/T) in the promoter regions of target genes (Rushton et al., 1996; Yu et al., 2001; Eulgem and Somssich, 2007; Lippok et al., 2007). The WRKY family transcription factor member WRKY33, a pathogen-inducible transcription factor, is a direct phosphorylation target of MPK3 and MPK6 (Mao et al., 2011). In *N. benthamiana*, *RbohA* and *RbohB*, the putative orthologs of Arabidopsis *RbohF* and *RbohD*, are essential for H_2O_2 production in the response against the oomycete pathogen *Phytophthora infestans* (Yoshioka et al., 2003). The *RbohB* promoter contains a functional W-box, and W-boxes are well known cis-regulatory elements recognized by WRKY transcription factors (Eulgem et al., 2000; Adachi et al., 2015). The expression of *WRKY33* was rapidly induced by Vd-toxins, and the transcription factor was directly involved in the activation of *AtRbohD* expression. In addition, it is required for H2Bub1 to regulate *AtRbohD*-dependent H_2O_2 signaling in the defense response to Vd-toxins. A positive regulatory loop, consisting of MPK3/6-WRKY33-ALD1-pipecolic acid, is a critical regulatory mechanism of systemic acquired resistance induction in Arabidopsis (Wang et al., 2018).

In conclusion, our results demonstrate that HUB-mediated H2Bub1 is involved in the regulation of defense responses against Vd-toxins through the transcriptional activation of the NADPH oxidase *AtRbohD* and *WRKY33*. H2Bub1 is associated with H3K4me3 deposition during the transcription induction of *AtRbohD* and *WRKY33*. The active transcription of WRKY33 regulates *AtRbohD* expression, and *AtRbohD*-dependent H_2O_2 signaling is a critical modulator in the defense response against Vd-toxins. In addition, H2Bub1 also affects posttranscriptional MAPK signaling. H2Bub1 is required for the activation of MPK3 and MPK6. Moreover, MPK3 and MPK6 associate with PTPs, which negatively regulated H_2O_2 production. The PTP-MPK3/6-WRKY pathway regulates H_2O_2 signaling in the response against Vd-toxins in Arabidopsis (Fig. 9).

MATERIALS AND METHODS

Plant Materials and Growth Conditions

Arabidopsis (*Arabidopsis thaliana*) Columbia-0 was used as the wild-type. Arabidopsis mutants and transgenic lines, *hub1-4*, *hub2-2*, *hub1-4 hub2-2*, *HUB1/hub1-4* (Cao et al., 2008), *rbohd*, *rbohf*, *rbohd/f* (Torres et al., 2002), *mpk3*, *mpk6*, *35S:MPK3*, *35S:MPK6*, *MKK5^{DD}* (Liu et al., 2008), *ptp1*, *mkp1*, *35S:PTP1*, and *35S:MKP1* (Zhou et al., 2017), were previously described.

The seeds were sterilized with 0.2% (v/v) sodium hypochlorite for 20 min, rinsed with water, and grown on one-half-strength MS medium supplemented with 1% (w/v) Suc and 0.8% (w/v) agar at 16°C or 22°C with a 16-h-light/8-h-dark cycle and 70% relative humidity in a growth cabinet.

Preparation of Crude Vd-Toxins

A highly infectious and defoliating strain of *Verticillium dahliae* (Vd991) was used to extract Vd-toxins. The *Verticillium* spp. culture filtrate was purified as described previously (Jia et al., 2007; Shi and Li, 2008). The fungal culture was filtered through filter paper, and the filtrate was centrifuged at 10,000*g* for 30 min to remove the spores. The supernatant was frozen (−20°C) for 24 h, lyophilized for 36 h, and dissolved in distilled water to make a 0.5 mg mL^{-1} solution. The solution was dialyzed using 1-kD dialysis membranes (MWCO) in 4°C for 24 h. The concentrated solution was frozen and lyophilized again, and the powder was dissolved in distilled water. The solution was then refiltered through a 0.45-μm Millipore filter. The resulting filtrate was used as crude Vd-toxins extract for further experiments.

Vd-Toxin Treatment Assays

For the phenotypic analysis, seeds of the wild type and the *hub1-4*, *hub2-2*, *hub1-4 hub2-2*, and *HUB1/hub1-4* mutants were germinated on one-half-strength MS medium for 4 d and then transplanted onto plates supplemented with Vd-toxins (100–300 μg mL^{-1}) and grown for another 4 d. For root length determinations after exposure to Vd-toxins, the root length of untreated seedlings of each genotype was set at 100%, and the mean values ± SD were shown as percentages of root length of the respective controls. Three independent experiments were performed, and at least 30 seedlings of each genotype were measured in each experiment.

H_2O_2 Assays

For the H_2DCF-DA staining assay, 7-d-old seedlings were incubated in 10 mM MES-KCl buffer (pH 6) supplemented with 200 μg mL^{-1} Vd-toxins and 20 μM H_2DCF-DA for 20 min at room temperature. Then they were washed three times with 10 mM MES-KCl buffer (pH 6) to remove the excess H_2DCF-DA. Seedlings incubated in double distilled water were used as controls. Fluorescence was detected with a confocal laser scanning microscope (Zeiss LSM 710) using the following conditions: power 70%, excitation at 488 nm, and emission at 505 to 530 nm. This experiment was independently repeated at least three times.

H_2O_2 content was measured using the chromogenic peroxidase-coupled assay (Veljovic-Jovanovic et al., 2002). The reaction mixture consisted of 0.1 M phosphate buffer (pH 6.5), 3.3 mM 3-dimethylaminobenzoic acid, 0.07 mM 3-methyl-2-benzothiazolinonehydrazone, and 0.1 unit mL^{-1} peroxidase (Sigma). The 7-d-old seedlings were treated with 200 μg mL^{-1} Vd-toxins, then 0.1 g of the leaves was ground to a fine powder in liquid nitrogen, and the powder was extracted in 2 mL of 1 M $HClO_4$. When required, the extractions were performed in the presence of insoluble 5% (w/v) polyvinylpyrrolidone. Homogenates were centrifuged at 12,000*g* for 10 min, and the supernatants were neutralized with 5 M K_2CO_3 to pH 5.6 in the presence of 100 μL of 0.3 M phosphate buffer (pH 5.6). The homogenates were then centrifuged at 12,000*g* for 1 min to remove $KClO_4$. When required, the sample was incubated prior to the assay for 10 min with 1 unit of ascorbate oxidase (Sigma) to oxidize ascorbate. The reaction was initiated by the addition of 200 μL of the sample and 2,700 μL of the reaction mixture. The absorbance change at 590 nm was monitored at 25°C. Three independent experiments were performed, each with three replicates, and similar results were obtained.

Detection of Cell Death in Leaves

Cell death in leaves was determined by staining them with Trypan Blue according to the method of Bowling et al. (1997). The experiments were repeated at least three times.

RT-qPCR

Arabidopsis total RNA was isolated using TRIzol reagent (Invitrogen) and treated with DNaseI according to the manufacturer's specifications (Invitrogen). For the RT-qPCR analysis, first-strand cDNA was synthesized from 1 μg of total RNA using PrimeScript reverse transcription reagents kit (TaKaRa). RT-qPCR was performed on an ABI 7500 Sequence Detector (Applied Biosystems) using the SYBR Premix Ex Taq Kit (TaKaRa) with gene-specific primers and the internal control (*ACTIN2*). The gene-specific primer pairs are listed in Supplemental Table S1. cDNA aliquots of 2 μL were amplified in a 25-μL reaction volume containing SYBR Premix Ex Taq, PCR forward primer, PCR reverse primer, and the ROX reference dye in accordance with the manufacturer's instructions (TaKaRa). PCR was conducted at 95°C for 30 s, followed by 40 cycles of 95°C for 5 s (denaturation) and annealing at 60°C for 34 s. Data analysis, including the determination of the threshold cycle that represents the starting point of the exponential phase of PCR, and graphic presentation were conducted using Sequence Detection Software version 1.07 (Applied Biosystems). The quantification of the transcript levels of the cDNA fragments was normalized to the expression of the *ACTIN2* gene in Arabidopsis at several points during the Vd-toxins treatment. Three independent experiments were performed, each with three replicates.

Yeast Two-Hybrid Assays

To create bait and prey plasmids, fragments were amplified by different primers and cloned into pGBKT7 and pGADT7, respectively. All the primer sequences are listed in Supplemental Table S1. MPK2-, MPK3-, and MPK6-coding sequences were independently cloned into the pGBKT7 vector (Clontech) as the bait constructs, while PTP1 and MKP1 were independently cloned into the pGADT7 vector (Clontech) as the prey constructs. Empty pGBKT7 and pGADT7 vectors were used as controls. Bait and prey constructs were cotransformed into *Saccharomyces cerevisiae* strain AH109. The transformants were tested on synthetic defined (SD) screening medium. Positive clones were identified by the ability to grow on the SD medium minus Leu/Trp/His/adenine and containing 6 mM 3-aminotriazole and 20 μg mL^{-1} 5-bromo-4-chloro-3-indolyl-β-D-galacto-pyranoside.

Yeast One-Hybrid Assays

The yeast one-hybrid assay was performed as described by Miao et al. (2004) and Li et al. (2010). The full-length cDNA of WRKY33 and DNA fragments of the *AtRbohD* promoter were amplified and independently cloned into pB42AD and pLacZi, respectively. All the primer sequences are listed in Supplemental Table S1. Empty pB42AD and pLacZi vectors were used as controls. The fusion constructs were cotransformed into *S. cerevisiae* strain EGY48. The transformants were tested on SD medium minus uracil and Leu and containing 20 μg mL^{-1} 5-bromo-4-chloro-3-indolyl-β-D-galacto-pyranoside.

GUS/LUC Assays

The transient GUS/LUC assay was performed as described by Zhao et al. (2016). The pCAMBIA1391 vector containing the Pro-35S:WRKY33 or Pro-RbohD:GUS construct was transfected into *Agrobacterium tumefaciens* strain GV3101. All the primer sequences are listed in Supplemental Table S1. Then, disposable sterilized syringes were used to inject these two bacterial solutions into different positions on the same *Nicotiana benthamiana* leaf. Empty vectors were used as controls. Three days after injection, the treated leaves were collected to measure the GUS and LUC activity levels. Methyl umbelliferyl glucuronide (Sigma) was used in the test of the GUS activity. The binding activity of WRKY33 to the *AtRbohD* promoter was determined by the GUS-to-LUC ratio.

EMSA

EMSA was performed as described in the protocol of the LightShift EMSA Optimization Control Kit (Thermo). The EMSA protocol of Zhao et al. (2016) was also referenced. All the primer sequences are listed in Supplemental Table S1. The recombinant proteins WRKY33-His and His were expressed and purified from *Escherichia coli* (BL21). Biotin-labeled or unlabeled primers were used to obtain two fragments (P1 and P2) of the *RbohD* promoter by PCR amplification. The unlabeled fragments and His protein were used as competitors and negative control, respectively.

ChIP Assays

ChIP was performed as described by Zhao et al. (2019) using 3-week-old seedlings. The anti-H2Bub1, anti-H3K4me3, and anti-H3 antibodies were purchased from Cell Signaling Technology. ChIP-qPCR was performed to analyze the enrichment of H2Bub1 and H3K4me3 in DNA fragments with anti-H2Bub1 anti-H3K4me3 antibodies, and anti-H3 antibodies were used to normalize H2Bub1 and H3K4me3 levels to nucleosome occupancy. As the H2Bub1 and H3K4me3 levels in *ACTIN2* chromatin were similar among *hub1-4*, *hub2-2*, and the wild type, *ACTIN2* was used as an internal control. The primers are provided in Supplemental Table S1.

Immunoblotting and MAPK Analyses

The 7-d-old Arabidopsis seedlings were treated with 200 μg mL^{-1} Vd-toxins at several time points and carefully placed into centrifuge tubes. Protein extraction buffer (100 mM HEPES, pH 7.5, 5 mM EDTA, 5 mM EGTA, 2 mM DTT, 10 mM Na_3VO_4, 10 mM NaF, 50 mM β-glycerolphosphate, 1 mM phenylmethylsulfonyl fluoride, 1 mM proteinase inhibitor cocktail and phosphatase inhibitor cocktail, 10% [w/v] glycerol, and 1% [w/v] polyvinylpolypyrrolidone) was added to resuspend each sample. After centrifugation at 10,000*g* for 30 min at 4°C, supernatants were transferred into clean tubes. The protein concentrations were determined using the Bio-Rad protein assay kit (Bio-Rad) with BSA as the standard.

For western-blot analysis, 30 μg of total protein per lane was separated on an 8% SDS-PAGE gel. After electrophoresis, the proteins were transferred onto polyvinylidene difluoride membranes. After blocking for 2 h in Tris-buffered saline plus Tween 20 buffer with 5% (w/v) BSA at room temperature, the membranes were incubated with anti-phospho-p44/42 MAPK (1:1,000; Cell Signaling Technology), anti-AtMPK3 (1:2,000; Sigma), and anti-AtMPK6 (1:2,000; Sigma) as primary antibodies and peroxidase-conjugated goat anti-rabbit IgG (1:2,000; Cell Signaling Technology) as the secondary antibody. Then the membranes were visualized using enhanced chemiluminescence substrate (ThermoFisher).

Co-IP Assays

Co-IP assays were performed as described previously (Ding et al., 2015). Transgenic plants independently harboring *35S:PTP1* and *35S:MKP1* and expressing PTP1-MYC and MKP1-MYC, respectively, were used to detect the interactions of MPK3/6 and PTP1/MKP1. Wild-type plants were used as the negative control. The total proteins extracted from wild-type and stable transgenic plants were independently immunoprecipitated with anti-Myc agarose (Sigma), anti-AtMPK3 (Sigma), and anti-AtMPK6 (Sigma). The immunoprecipitates were separated on a 10% SDS-PAGE gel and detected with corresponding antibodies. Then, the membranes were visualized using an enhanced chemiluminescence substrate (ThermoFisher).

Statistical Analyses

Statistical data were analyzed by SPSS statistics software. Data were analyzed by one-way ANOVA with Tukey's honestly significant difference posthoc tests. Values of $P < 0.05$ are noted in the figure legends, and significant differences are indicated by different letters.

Accession Numbers

Sequence data for the genes described in this article can be found in TAIR (https://www.arabidopsis.org/) with the following accession numbers: AT2G44950 for *HUB1*, AT1G55250 for *HUB2*, AT5G47910 for *AtRbohD*, AT1G64060 for *AtRbohF*, AT2G14610 for *PR1*, AT2G38470 for *WRKY33*, AT1G02930 for *GST1*, AT3G45640 for *MPK3*, AT2G43790 for *MPK6*, AT1G71860 for *PTP1*, and AT3G55270 for *MKP1*.

Supplemental Data

The following supplemental materials are available.

Supplemental Figure S1. Global change in H2Bub1 induced by the Vd-toxins treatment in wild-type Arabidopsis.

Supplemental Figure S2. Kinase activity levels of MPK3 and MPK6 detected in wild-type, *mpk3*, and *mpk6* Arabidopsis plants.

Supplemental Table S1. Primers used in this work.

ACKNOWLEDGMENTS

We thank Dr. Ligeng Ma (Capital Normal University, Beijing) for the *hub1-4*, *hub2-2*, and *hub1-4 hub2-2* mutants and the *HUB1/hub1-4* complementation line, Dr. Miguel A. Torres (University of North Carolina, Chapel Hill) for the *rbohD*, *rbohF*, and *rbohD/F* mutants, and Dr. Dongtao Ren (China Agricultural University, Beijing) for the *mpk3*, *mpk6*, *35S:MPK3*, *35S:MPK6*, and $MKK5^{DD}$ mutants.

Received July 30, 2019; accepted October 18, 2019; published October 30, 2019.

LITERATURE CITED

Adachi H, Nakano T, Miyagawa N, Ishihama N, Yoshioka M, Katou Y, Yaeno T, Shirasu K, Yoshioka H (2015) WRKY transcription factors phosphorylated by MAPK regulate a plant immune NADPH oxidase in *Nicotiana benthamiana*. Plant Cell **27:** 2645–2663

Anderson JC, Bartels S, González Besteiro MA, Shahollari B, Ulm R, Peck SC (2011) *Arabidopsis* MAP Kinase Phosphatase 1 (AtMKP1) negatively regulates MPK6-mediated PAMP responses and resistance against bacteria. Plant J **67:** 258–268

Apel K, Hirt H (2004) Reactive oxygen species: Metabolism, oxidative stress, and signal transduction. Annu Rev Plant Biol **55:** 373–399

Asai S, Ohta K, Yoshioka H (2008) MAPK signaling regulates nitric oxide and NADPH oxidase-dependent oxidative bursts in *Nicotiana benthamiana*. Plant Cell **20:** 1390–1406

Asai T, Tena G, Plotnikova J, Willmann MR, Chiu WL, Gomez-Gomez L, Boller T, Ausubel FM, Sheen J (2002) MAP kinase signalling cascade in *Arabidopsis* innate immunity. Nature **415:** 977–983

Bartels S, Anderson JC, González Besteiro MA, Carreri A, Hirt H, Buchala A, Métraux JP, Peck SC, Ulm R (2009) MAP kinase phosphatase1 and protein tyrosine phosphatase1 are repressors of salicylic acid synthesis and SNC1-mediated responses in *Arabidopsis*. Plant Cell **21:** 2884–2897

Beckers GJ, Jaskiewicz M, Liu Y, Underwood WR, He SY, Zhang S, Conrath U (2009) Mitogen-activated protein kinases 3 and 6 are required for full priming of stress responses in *Arabidopsis thaliana*. Plant Cell **21:** 944–953

Bhat RG, Subbarao KV (1999) Host range specificity in *Verticillium dahliae*. Phytopathology **89:** 1218–1225

Birkenbihl RP, Diezel C, Somssich IE (2012) *Arabidopsis* WRKY33 is a key transcriptional regulator of hormonal and metabolic responses toward *Botrytis cinerea* infection. Plant Physiol **159:** 266–285

Boller T, Felix G (2009) A renaissance of elicitors: Perception of microbe-associated molecular patterns and danger signals by pattern-recognition receptors. Annu Rev Plant Biol **60:** 379–406

Bourbousse C, Ahmed I, Roudier F, Zabulon G, Blondet E, Balzergue S, Colot V, Bowler C, Barneche F (2012) Histone H2B monoubiquitination facilitates the rapid modulation of gene expression during *Arabidopsis* photomorphogenesis. PLoS Genet **8:** e1002825

Bowling SA, Clarke JD, Liu Y, Klessig DF, Dong X (1997) The *cpr5* mutant of *Arabidopsis* expresses both NPR1-dependent and NPR1-independent resistance. Plant Cell **9:** 1573–1584

Cao H, Li X, Wang Z, Ding M, Sun Y, Dong F, Chen F, Liu L, Doughty J, Li Y, et al (2015) Histone H2B monoubiquitination mediated by HISTONE MONOUBIQUITINATION1 and HISTONE MONOUBIQUITINATION2 is involved in anther development by regulating tapetum degradation-related genes in rice. Plant Physiol **168:** 1389–1405

Cao Y, Dai Y, Cui S, Ma L (2008) Histone H2B monoubiquitination in the chromatin of FLOWERING LOCUS C regulates flowering time in Arabidopsis. Plant Cell **20:** 2586–2602

Chaouch S, Queval G, Noctor G (2012) AtRbohF is a crucial modulator of defence-associated metabolism and a key actor in the interplay between intracellular oxidative stress and pathogenesis responses in *Arabidopsis*. Plant J **69:** 613–627

Chen P, Hutter D, Yang X, Gorospe M, Davis RJ, Liu Y (2001) Discordance between the binding affinity of mitogen-activated protein kinase subfamily members for MAP kinase phosphatase-2 and their ability to activate the phosphatase catalytically. J Biol Chem **276:** 29440–29449

Dangl JL, Jones JDG (2001) Plant pathogens and integrated defence responses to infection. Nature **411:** 826–833

Dhawan R, Luo H, Foerster AM, Abuqamar S, Du HN, Briggs SD, Mittelsten Scheid O, Mengiste T (2009) HISTONE MONOUBIQUITINATION1 interacts with a subunit of the mediator complex and regulates defense against necrotrophic fungal pathogens in *Arabidopsis*. Plant Cell **21:** 1000–1019

Ding Y, Li H, Zhang X, Xie Q, Gong Z, Yang S (2015) OST1 kinase modulates freezing tolerance by enhancing ICE1 stability in Arabidopsis. Dev Cell **32:** 278–289

Eulgem T, Rushton PJ, Robatzek S, Somssich IE (2000) The WRKY superfamily of plant transcription factors. Trends Plant Sci **5:** 199–206

Eulgem T, Somssich IE (2007) Networks of WRKY transcription factors in defense signaling. Curr Opin Plant Biol **10:** 366–371

Feng J, Shen WH (2014) Dynamic regulation and function of histone monoubiquitination in plants. Front Plant Sci **5:** 83

Fiorucci AS, Bourbousse C, Concia L, Rougée M, Deton-Cabanillas AF, Zabulon G, Layat E, Latrasse D, Kim SK, Chaumont N, et al (2019) Arabidopsis S2Lb links AtCOMPASS-like and SDG2 activity in H3K4me3 independently from histone H2B monoubiquitination. Genome Biol **20:** 100–121

Fleury D, Himanen K, Cnops G, Nelissen H, Boccardi TM, Maere S, Beemster GT, Neyt P, Anami S, Robles P, et al (2007) The *Arabidopsis thaliana* homolog of yeast *BRE1* has a function in cell cycle regulation during early leaf and root growth. Plant Cell **19:** 417–432

Fradin EF, Thomma BP (2006) Physiology and molecular aspects of *Verticillium* wilt diseases caused by *V. dahliae* and *V. albo-atrum*. Mol Plant Pathol **7:** 71–86

Gadjev I, Vanderauwera S, Gechev TS, Laloi C, Minkov IN, Shulaev V, Apel K, Inzé D, Mittler R, Van Breusegem F (2006) Transcriptomic footprints disclose specificity of reactive oxygen species signaling in *Arabidopsis*. Plant Physiol **141:** 436–445

Ghelis T, Bolbach G, Clodic G, Habricot Y, Miginiac E, Sotta B, Jeannette E (2008) Protein tyrosine kinases and protein tyrosine phosphatases are involved in abscisic acid-dependent processes in *Arabidopsis* seeds and suspension cells. Plant Physiol **148:** 1668–1680

Greenberg JT, Yao N (2004) The role and regulation of programmed cell death in plant-pathogen interactions. Cell Microbiol **6:** 201–211

Gu X, Jiang D, Wang Y, Bachmair A, He Y (2009) Repression of the floral transition via histone H2B monoubiquitination. Plant J **57:** 522–533

Himanen K, Woloszynska M, Boccardi TM, De Groeve S, Nelissen H, Bruno L, Vuylsteke M, Van Lijsebettens M (2012) Histone H2B monoubiquitination is required to reach maximal transcript levels of circadian clock genes in *Arabidopsis*. Plant J **72:** 249–260

Hu M, Pei BL, Zhang LF, Li YZ (2014) Histone H2B monoubiquitination is involved in regulating the dynamics of microtubules during the defense response to *Verticillium dahliae* toxins in Arabidopsis. Plant Physiol **164:** 1857–1865

Ichimura K, Shinozaki K, Tena G, Sheen J, Henry Y, Champion A, Kreis M, Zhang SQ, Hirt H, Wilson C, et al (2002) Mitogen-activated protein kinase cascades in plants: A new nomenclature. Trends Plant Sci **7:** 301–308

Ishihama N, Yoshioka H (2012) Post-translational regulation of WRKY transcription factors in plant immunity. Curr Opin Plant Biol **15:** 431–437

Jia ZQ, Yuan HY, Li YZ (2007) NO and H_2O_2 induced by *Verticillium dahliae* toxins and its influence on expression of *GST* gene in cotton suspension cells. Chin Sci Bull **52:** 1347–1354

Lamb C, Dixon RA (1997) The oxidative burst in plant disease resistance. Annu Rev Plant Physiol Plant Mol Biol **48:** 251–275

Lee JS, Shukla A, Schneider J, Swanson SK, Washburn MP, Florens L, Bhaumik SR, Shilatifard A (2007) Histone crosstalk between H2B monoubiquitination and H3 methylation mediated by COMPASS. Cell **131:** 1084–1096

Lee S, Fu F, Xu S, Lee SY, Yun DJ, Mengiste T (2016) Global regulation of plant immunity by histone lysine methyl transferases. Plant Cell **28:** 1640–1661

Li B, Carey M, Workman JL (2007) The role of chromatin during transcription. Cell **128:** 707–719

Li J, Li G, Gao S, Martinez C, He G, Zhou Z, Huang X, Lee JH, Zhang H, Shen Y, et al (2010) Arabidopsis transcription factor ELONGATED

HYPOCOTYL5 plays a role in the feedback regulation of phytochrome A signaling. Plant Cell **22:** 3634–3649

Lin W, Li B, Lu D, Chen S, Zhu N, He P, Shan L (2014) Tyrosine phosphorylation of protein kinase complex BAK1/BIK1 mediates *Arabidopsis* innate immunity. Proc Natl Acad Sci USA **111:** 3632–3637

Lippok B, Birkenbihl RP, Rivory G, Brümmer J, Schmelzer E, Logemann E, Somssich IE (2007) Expression of *AtWRKY33* encoding a pathogen- or PAMP-responsive WRKY transcription factor is regulated by a composite DNA motif containing W box elements. Mol Plant Microbe Interact **20:** 420–429

Liu H, Wang Y, Xu J, Su T, Liu G, Ren D (2008) Ethylene signaling is required for the acceleration of cell death induced by the activation of AtMEK5 in Arabidopsis. Cell Res **18:** 422–432

Liu S, Ziegler J, Zeier J, Birkenbihl RP, Somssich IE (2017) *Botrytis cinerea* B05.10 promotes disease development in *Arabidopsis* by suppressing WRKY33-mediated host immunity. Plant Cell Environ **40:** 2189–2206

Liu Y, Koornneef M, Soppe WJ (2007) The absence of histone H2B monoubiquitination in the *Arabidopsis hub1* (*rdo4*) mutant reveals a role for chromatin remodeling in seed dormancy. Plant Cell **19:** 433–444

Love AJ, Yun BW, Laval V, Loake GJ, Milner JJ (2005) *Cauliflower mosaic virus*, a compatible pathogen of Arabidopsis, engages three distinct defense-signaling pathways and activates rapid systemic generation of reactive oxygen species. Plant Physiol **139:** 935–948

Macho AP, Schwessinger B, Ntoukakis V, Brutus A, Segonzac C, Roy S, Kadota Y, Oh MH, Sklenar J, Derbyshire P, et al (2014) A bacterial tyrosine phosphatase inhibits plant pattern recognition receptor activation. Science **343:** 1509–1512

Malapeira J, Khaitova LC, Mas P (2012) Ordered changes in histone modifications at the core of the *Arabidopsis* circadian clock. Proc Natl Acad Sci USA **109:** 21540–21545

Mao G, Meng X, Liu Y, Zheng Z, Chen Z, Zhang S (2011) Phosphorylation of a WRKY transcription factor by two pathogen-responsive MAPKs drives phytoalexin biosynthesis in *Arabidopsis*. Plant Cell **23:** 1639–1653

Marino D, Dunand C, Puppo A, Pauly N (2012) A burst of plant NADPH oxidases. Trends Plant Sci **17:** 9–15

Ménard R, Verdier G, Ors M, Erhardt M, Beisson F, Shen WH (2014) Histone H2B monoubiquitination is involved in the regulation of cutin and wax composition in *Arabidopsis thaliana*. Plant Cell Physiol **55:** 455–466

Miao Y, Laun T, Zimmermann P, Zentgraf U (2004) Targets of the WRKY53 transcription factor and its role during leaf senescence in *Arabidopsis*. Plant Mol Biol **55:** 853–867

Miller G, Schlauch K, Tam R, Cortes D, Torres MA, Shulaev V, Dangl JL, Mittler R (2009) The plant NADPH oxidase RBOHD mediates rapid systemic signaling in response to diverse stimuli. Sci Signal **2:** ra45

Mittler R, Vanderauwera S, Suzuki N, Miller G, Tognetti VB, Vandepoele K, Gollery M, Shulaev V, Van Breusegem F (2011) ROS signaling: The new wave? Trends Plant Sci **16:** 300–309

Morales J, Kadota Y, Zipfel C, Molina A, Torres MA (2016) The *Arabidopsis* NADPH oxidases RbohD and RbohF display differential expression patterns and contributions during plant immunity. J Exp Bot **67:** 1663–1676

Nemoto K, Takemori N, Seki M, Shinozaki K, Sawasaki T (2015) Members of the plant CRK superfamily are capable of trans- and autophosphorylation of tyrosine residues. J Biol Chem **290:** 16665–16677

Pandey SP, Somssich IE (2009) The role of WRKY transcription factors in plant immunity. Plant Physiol **150:** 1648–1655

Pavri R, Zhu B, Li G, Trojer P, Mandal S, Shilatifard A, Reinberg D (2006) Histone H2B monoubiquitination functions cooperatively with FACT to regulate elongation by RNA polymerase II. Cell **125:** 703–717

Pedley KF, Martin GB (2005) Role of mitogen-activated protein kinases in plant immunity. Curr Opin Plant Biol **8:** 541–547

Pitzschke A (2015) Modes of MAPK substrate recognition and control. Trends Plant Sci **20:** 49–55

Pitzschke A, Hirt H (2009) Disentangling the complexity of mitogen-activated protein kinases and reactive oxygen species signaling. Plant Physiol **149:** 606–615

Rodriguez MC, Petersen M, Mundy J (2010) Mitogen-activated protein kinase signaling in plants. Annu Rev Plant Biol **61:** 621–649

Rushton PJ, Torres JT, Parniske M, Wernert P, Hahlbrock K, Somssich IE (1996) Interaction of elicitor-induced DNA-binding proteins with elicitor response elements in the promoters of parsley PR1 genes. EMBO J **15:** 5690–5700

Sang Y, Macho AP (2017) Analysis of PAMP-triggered ROS burst in plant immunity. Methods Mol Biol **1578:** 143–153

Schmitz RJ, Tamada Y, Doyle MR, Zhang X, Amasino RM (2009) Histone H2B deubiquitination is required for transcriptional activation of FLOWERING LOCUS C and for proper control of flowering in Arabidopsis. Plant Physiol **149:** 1196–1204

Segonzac C, Feike D, Gimenez-Ibanez S, Hann DR, Zipfel C, Rathjen JP (2011) Hierarchy and roles of pathogen-associated molecular pattern-induced responses in *Nicotiana benthamiana*. Plant Physiol **156:** 687–699

Shaban M, Miao Y, Ullah A, Khan AQ, Menghwar H, Khan AH, Ahmed MM, Tabassum MA, Zhu L (2018) Physiological and molecular mechanism of defense in cotton against *Verticillium dahliae*. Plant Physiol Biochem **125:** 193–204

Shi FM, Li YZ (2008) Verticillium dahliae toxins-induced nitric oxide production in Arabidopsis is major dependent on nitrate reductase. BMB Rep **41:** 79–85

Suzuki N, Miller G, Morales J, Shulaev V, Torres MA, Mittler R (2011) Respiratory burst oxidases: The engines of ROS signaling. Curr Opin Plant Biol **14:** 691–699

Tamnanloo F, Damen H, Jangra R, Lee JS (2018) MAP KINASE PHOSPHATASE1 controls cell fate transition during stomatal development. Plant Physiol **178:** 247–257

Tena G, Asai T, Chiu WL, Sheen J (2001) Plant mitogen-activated protein kinase signaling cascades. Curr Opin Plant Biol **4:** 392–400

Torres MA, Dangl JL (2005) Functions of the respiratory burst oxidase in biotic interactions, abiotic stress and development. Curr Opin Plant Biol **8:** 397–403

Torres MA, Dangl JL, Jones JDG (2002) Arabidopsis gp91phox homologues AtrbohD and AtrbohF are required for accumulation of reactive oxygen intermediates in the plant defense response. Proc Natl Acad Sci USA **99:** 517–522

Torres MA, Jones JDG, Dangl JL (2005) Pathogen-induced, NADPH oxidase-derived reactive oxygen intermediates suppress spread of cell death in *Arabidopsis thaliana*. Nat Genet **37:** 1130–1134

Torres MA, Jones JDG, Dangl JL (2006) Reactive oxygen species signaling in response to pathogens. Plant Physiol **141:** 373–378

Veljovic-Jovanovic S, Novtor G, Foyer CH (2002) Are leaf hydrogen peroxide concentrations commonly overestimated? The potential influence of artefactual interference by tissue phenolics and ascorbate. Plant Physiol Biochem **40:** 501–507

Wang Y, Schuck S, Wu J, Yang P, Döring AC, Zeier J, Tsuda K (2018) A MPK3/6-WRKY33-ALD1-pipecolic acid regulatory loop contributes to systemic acquired resistance. Plant Cell **30:** 2480–2494

Weake VM, Workman JL (2008) Histone ubiquitination: Triggering gene activity. Mol Cell **29:** 653–663

Xu J, Xie J, Yan C, Zou X, Ren D, Zhang S (2014) A chemical genetic approach demonstrates that MPK3/MPK6 activation and NADPH oxidase-mediated oxidative burst are two independent signaling events in plant immunity. Plant J **77:** 222–234

Xu L, Ménard R, Berr A, Fuchs J, Cognat V, Meyer D, Shen WH (2009) The E2 ubiquitin-conjugating enzymes, AtUBC1 and AtUBC2, play redundant roles and are involved in activation of FLC expression and repression of flowering in Arabidopsis thaliana. Plant J **57:** 279–288

Yao LL, Zhou Q, Pei BL, Li YZ (2011) Hydrogen peroxide modulates the dynamic microtubule cytoskeleton during the defence responses to Verticillium dahliae toxins in Arabidopsis. Plant Cell Environ **34:** 1586–1598

Yoshioka H, Numata N, Nakajima K, Katou S, Kawakita K, Rowland O, Jones JD, Doke N (2003) *Nicotiana benthamiana* gp91^{phox} homologs *NbrbohA* and *NbrbohB* participate in H_2O_2 accumulation and resistance to *Phytophthora infestans*. Plant Cell **15:** 706–718

Yu D, Chen C, Chen Z (2001) Evidence for an important role of WRKY DNA binding proteins in the regulation of *NPR1* gene expression. Plant Cell **13:** 1527–1540

Zhang J, Shao F, Li Y, Cui H, Chen L, Li H, Zou Y, Long C, Lan L, Chai J, et al (2007) A *Pseudomonas syringae* effector inactivates MAPKs to suppress PAMP-induced immunity in plants. Cell Host Microbe **1:** 175–185

Zhang S, Klessig DF (2001) MAPK cascades in plant defense signaling. Trends Plant Sci **6:** 520–527

Zhao S, Zhang ML, Ma TL, Wang Y (2016) Phosphorylation of ARF2 relieves its repression of transcription of the K^+ transporter gene *HAK5* in response to low potassium stress. Plant Cell **28:** 3005–3019

Zhao W, Neyt P, Van Lijsebettens M, Shen WH, Berr A (2019) Interactive and noninteractive roles of histone H2B monoubiquitination and H3K36 methylation in the regulation of active gene transcription and control of plant growth and development. New Phytol **221:** 1101–1116

Zheng Z, Qamar SA, Chen Z, Mengiste T (2006) *Arabidopsis* WRKY33 transcription factor is required for resistance to necrotrophic fungal pathogens. Plant J **48:** 592–605

Zhou S, Chen Q, Sun Y, Li Y (2017) Histone H2B monoubiquitination regulates salt stress-induced microtubule depolymerization in *Arabidopsis*. Plant Cell Environ **40:** 1512–1530

Zou B, Yang DL, Shi Z, Dong H, Hua J (2014) Monoubiquitination of histone 2B at the disease resistance gene locus regulates its expression and impacts immune responses in Arabidopsis. Plant Physiol **165:** 309–318